AFML-TR-65-2
PART II, VOLUME XVIII

TERNARY PHASE EQUILIBRIA IN TRANSITION METAL-BORON-CARBON-SILICON SYSTEMS

PART II. TERNARY SYSTEMS
VOLUME XVIII. CONSTITUTION OF NIOBIUM-TUNGSTEN-CARBON ALLOYS

E. RUDY

Aerojet-General Corporation

TECHNICAL REPORT AFML-TR-65-2, PART II, VOLUME XVIII

JANUARY 1969

AIR FORCE MATERIALS LABORATORY
AIR FORCE SYSTEMS COMMAND
WRIGHT-PATTERSON AIR FORCE BASE, OHIO

NOTICES

When Government drawings, specifications, or other data are used for any purpose other than in connection with a definitely related Government procurement operation, the United States Government thereby incurs no responsibility nor any obligation whatsoever; and the fact that the Government may have formulated, furnished, or in any way supplied the said drawings, specifications, or other data, is not to be regarded by implication or otherwise as in any manner licensing the holder or any other person or corporation, or conveying any rights or permission to manufacture, use or sell any patented invention that may in any way be related thereto.

This document has been approved for public release and sale; its distribution is unlimited.

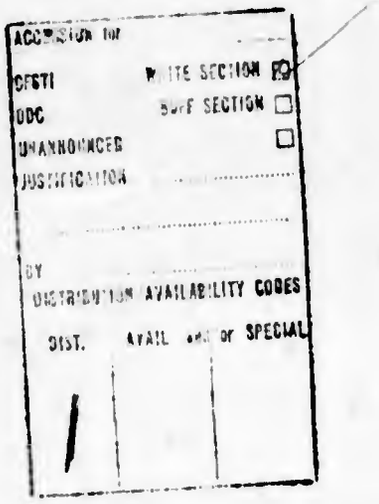

Copies of this report should not be returned unless return is required by security considerations, contractual obligations, or notice on a specific document.

500 - March 1969 - CO455 - 69-1515

BLANK PAGE

TERNARY PHASE EQUILIBRIA IN TRANSITION METAL-BORON-CARBON-SILICON SYSTEMS

PART II. TERNARY SYSTEMS

VOLUME XVIII. CONSTITUTION OF NIOBIUM-TUNGSTEN-CARBON ALLOYS

E. RUDY

FOREWORD

The research described in this report was carried out at the Materials Research Laboratory, Aerojet-General Corporation, Sacramento, California, under USAF Contract No. AF 33(615)-1249. The contract was initiated under Project No. 7350, Task No. 735001, and was administered under the direction of the Air Force Materials Laboratory, with Capt. P.J. Marchiando acting as Project Engineer, and Dr. E. Rudy, Aerojet-General Corporation, as Principal Investigator. Professor Dr. Hans Nowotny, University of Vienna, served as consultant to the project.

The project, which includes the experimental and theoretical investigations of ternary and related binary systems in the system classes Me_1-Me_2-C, Me-B-C, Me_1-Me_2-B, Me-Si-B, and Me-Si-C, was initiated on 1 January 1964. An extension effort to this contract commenced in January 1966.

The phase diagram work on the ternary system described in this report was carried by E. Rudy. Assisting in the investigations were: J. Hoffman (metallographic preparations), J. Pomodoro (sample preparation), and R. Cobb (X-ray exposures and photographic work).

Chemical analysis of the alloys was performed under the supervision of Mr. W.E. Trahan, Quality Control Division of Aerojet-General Corporation. The authors wish to thank Mr. R. Cristoni for the preparation of the illustrations, and Mrs. J. Weidner, who typed the report.

The manuscript of this report was released by the authors April 1968 for publication as a technical report.

Other reports issued under USAF contract AF 33(615)-1249 have included:

Part I. Related Binaries

Volume I.	Mo-C System
Volume II.	Ti-C and Zr-C Systems
Volume III.	Systems Mo-B and W-B
Volume IV.	Hf-C System
Volume V.	Ta-C System. Partial Investigations in the Systems V-C and Nb-C
Volume VI.	W-C System. Supplemental Information on the Mo-C System
Volume VII.	Ti-B System
Volume VIII.	Zr-B System
Volume IX.	Hf-B System
Volume X.	V-B, Nb-B, and Ta-B Systems
Volume XI.	Final Report on the Mo-C System
Volume XII.	Revision of the Vanadium-Carbon and Niobium-Carbon Systems

Volume XIII.	The Zirconium-Silicon and Hafnium-Silicon Systems
Volume XIV.	Constitution of the Hafnium-Vanadium and Hafnium-Chromium Systems

Part II. Ternary Systems

Volume I.	Ta-Hf-C System
Volume II.	Ti-Ta-C System
Volume III.	Zr-Ta-C System
Volume IV.	Ti-Zr-C, Ti-Hf-C, and Zr-Hf-C Systems
Volume V.	Ti-Hf-B System
Volume VI.	Zr-Hf-B System
Volume VII.	Systems Ti-Si-C, Nb-Si-C, and W-Si-C
Volume VIII.	Ta-W-C System
Volume IX.	Zr-W-B System. Pseudo-Binary System TaB_2-HfB_2
Volume X.	Systems Zr-Si-C, Hf-Si-C, Zr-Si-B, and Hf-Si-B
Volume XI.	Systems Hf-Mo-B and Hf-W-B
Volume XII.	Ti-Zr-B System
Volume XIII.	Phase Diagrams of the Systems Ti-B-C, Zr-B-C, and Hf-B-C
Volume XIV.	The Hafnium-Iridium-Boron System
Volume XV.	Constitution of Niobium-Molybdenum-Carbon Alloys
Volume XVI.	The Vanadium-Niobium-Carbon System
Volume XVII.	Constitution of Ternary Ta-Mo-C Alloys

Part III. Special Experimental Techniques

Volume I.	High Temperature Differential Thermal Analysis
Volume II.	A Pirani-Furnace for the Precision Determination of the Melting Temperatures of Refractory Metallic Substances

Part IV. Thermochemical Calculations

Volume I.	Thermodynamic Properties of Group IV, V, and VI Binary Transition Metal Carbides.
Volume II.	Thermodynamic Interpretation of Ternary Phase Diagrams
Volume III.	Computational Approaches to the Calculation of Ternary Phase Diagrams.

This technical report has been reviewed and is approved.

W. G. RAMKE
Chief, Ceramics and Graphite Branch
Metals and Ceramics Division
Air Force Materials Laboratory

ABSTRACT

The ternary alloy system niobium-tungsten-carbon was investigated by means of X-ray, melting point, DTA, and metallographic techniques on chemically and thermally defined specimens. A phase diagram from 1500°C through the melting range was established.

The solid state equilibria in the system are characterized by limited metal exchanges in the subcarbides and the occurrence of a two-phase equilibrium between the monocarbide and the metal phase. Above 2530°C, niobium monocarbide and the cubic high temperature phase in the W-C system form an uninterrupted series of solid solutions; below this temperature, the tungsten exchange in NbC is temperature-dependent and decreases to approximately 25 At.% W at 1500°C. The tungsten exchange in Nb_2C is less than 5 At.% at all temperatures, whereas the solubility in W_2C increases from ~ 24 mole % Nb_2C at 1500°C, to a maximum of approximately 37 mole % Nb_2C at 2600°C. The order-disorder reaction, as well as the change-of-order transition temperature in W_2C and Nb_2C are lowered by niobium additions, but the details of the transition reactions in the ternary could not be delineated.

Five isothermal reactions, all of which involve a liquid phase, occur in the system. Two correspond to limiting tie lines and the remaining three are class II (two-over-two) ternary reactions.

The results of this phase diagram investigation are discussed and the phase equilibria thermodynamically analyzed and interpreted.

TABLE OF CONTENTS

LIST OF FIGURES

LIST OF FIGURES (cont'd)

LIST OF FIGURES (cont'd)

LIST OF TABLES

BLANK PAGE

I. INTRODUCTION AND SUMMARY

A. INTRODUCTION

In previous investigations of ternary alloys involving combinations of group V with group VI transition metals and carbon, it was demonstrated that, in certain combinations, solid solutions or equilibria between the subcarbides are replaced by equilibria between the monocarbide and the metal phase. Such two-phase equilibria are, for example, found in the systems Nb(Ta)-Mo(W)-C[1-6], whereas in the corresponding systems with vanadium[7, 8] the subcarbides form continuous series of solid solutions. Differences, however, do also exist between the niobium and the tantalum-containing systems, inasmuch as the metal + monocarbide combinations remain stable up to solidus temperatures in the former,[2] whereas solid solution formation between the subcarbides becomes complete above certain temperatures in the tantalum-containing systems[3, 5].

The existence of two-phase equilibria of the type: metal + monocarbide in these systems is of special technical interest since this phase behavior allows the cementation of the monocarbides by refractory metal alloys without undesirable interference caused by the subcarbides in the boundary systems.

Although the disappearance of these two-phase equilibria in the tantalum-containing systems towards higher temperatures does appear undesirable at the first glance, a closer examination reveals that advantage can be taken of the pseudoeutectoid decomposition reaction of ternary subcarbide solutions to effectively control the grain size and, to a certain degree, the morphology of the metal and monocarbide phases resulting from the disproportionation.

Such means of grain size control could, for example, be important in the fabrication of special cutting tools, since the increase in performance of cemented carbide-based cutting tools with decreasing grain sizes of the constituents is well established and currently used mechanical

communication techniques as well as the sintering treatments during fabrication set a practical lower limit for the grain sizes which can be attained.

The main effort in the investigation of the W-C system concentrated on the delineation of the gross features of the ternary phase relationships at temperatures above 2000°C; special emphasis was devoted to the concentration space between the metal and monocarbide phase to determine whether or not complete solid solution formation between the subcarbides would occur at high temperatures and to study the effect of alloying upon the morphology of the binary Me + Me_2C eutectics.

B. SUMMARY

The phase equilibria in the niobium-tungsten carbon system are summarized as follows:

Above 2530°C, NbC and the cubic carbide in the tungsten-carbon system, α-WC_{1-x}, form a continuous series of solid solutions. The lattice parameter-concentration curve shows a slight positive deviation from a linear relationship between the values of the boundary phases (a = 4.470 Å for $NbC_{0.97}$, and a = 4.22$_0$ Å for $WC_{0.61}$). Below 2530°C, the tungsten exchange in NbC is temperature-dependent, decreasing from ~80 At.% W at 2200°C (a = 4.28 Å), to approximately 35 At.% W (a = 4.39 Å) at 1700°C. The maximum solidus temperatures of the monocarbide phase vary smoothly between the melting points of the boundary carbides (2747° for α-$WC_{0.64}$, 3615° for $NbC_{0.79}$).

The two-phase range (NbW) + $(Nb, W)C_{1-x}$ remains stable up to solidus temperatures, and both subcarbides are terminated by three-phase equilibria of the type Me + Me_2C + MeC_{1-x} towards the ternary phase field. The tungsten exchange in Nb_2C is less than 5 At.% at all temperatures, whereas W_2C exchanges up to ~38 At.% Nb (a = 2.997 Å, c = 4.727 Å for $WC_{0.47}$; a = 3.028 Å, c = 4.792 Å for the terminal solid solution at 2690°C).

The occurrence of five isothermal reactions, all of which involve a liquid phase, was ascertained. Two further solid state isotherms were indicated to result from the order-disorder transition in the Me_2C phases, but the equilibria involved were not studied in detail. The reaction isotherms, in the order of decreasing temperatures, are:

(1) 2860°C: $L + (Nb, W)C\text{-ss}_{1-x} \rightleftarrows W_2C\text{-ss}$ (pseudobinary peritectic formation of W_2C-phase)

(2) 2840°C: $L \rightleftarrows W_2C\text{-ss}$ change from peritectic to maximum type of melting of the subcarbide solid solution

(3) 2760°C: $L + \text{graphite} \rightleftarrows WC\text{-ss} + (Nb, W)C_{1-x}\text{-ss}$

(4) 2690°C: $L + W_2C\text{-ss} \rightleftarrows (Nb, W)\text{-ss} + (Nb, W)C_{1-x}\text{-ss}$

(5) 2490°C: $L + (Nb, W)C_{1-x} \rightleftarrows (Nb, W)\text{-ss} + Nb_2C\text{-ss}$

The isometric view of the phase diagram, shown for temperatures above 1500°C (Figure 1), is supplemented by the flow diagram of binary and ternary reactions (Figure 2) and the liquidus projections (Figure 3). The temperature sequence of the most important equilibria occurring in the system are depicted in the isopleth shown in Figure 4.

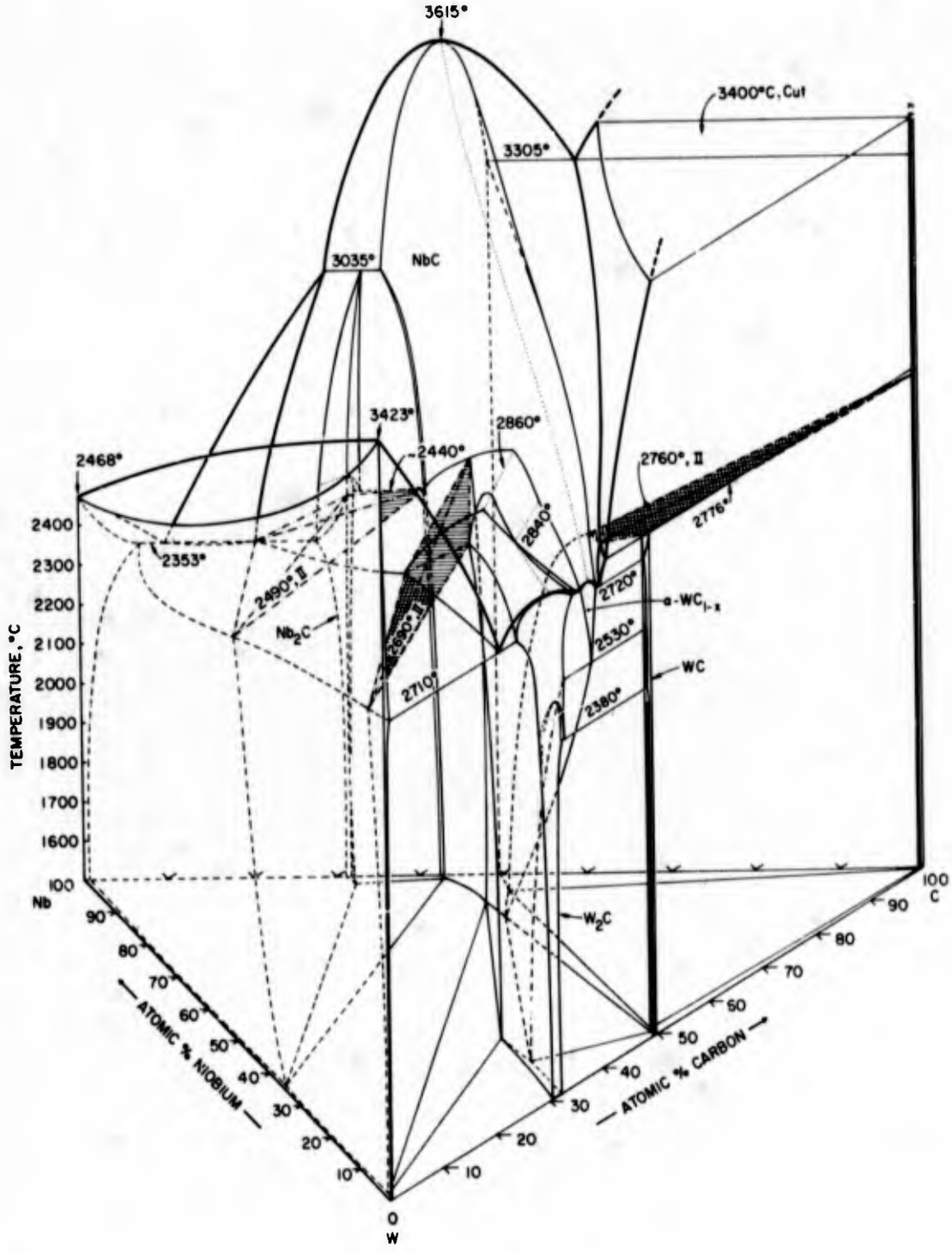

Figure 1. Isometric View of the Nb-W-C System.

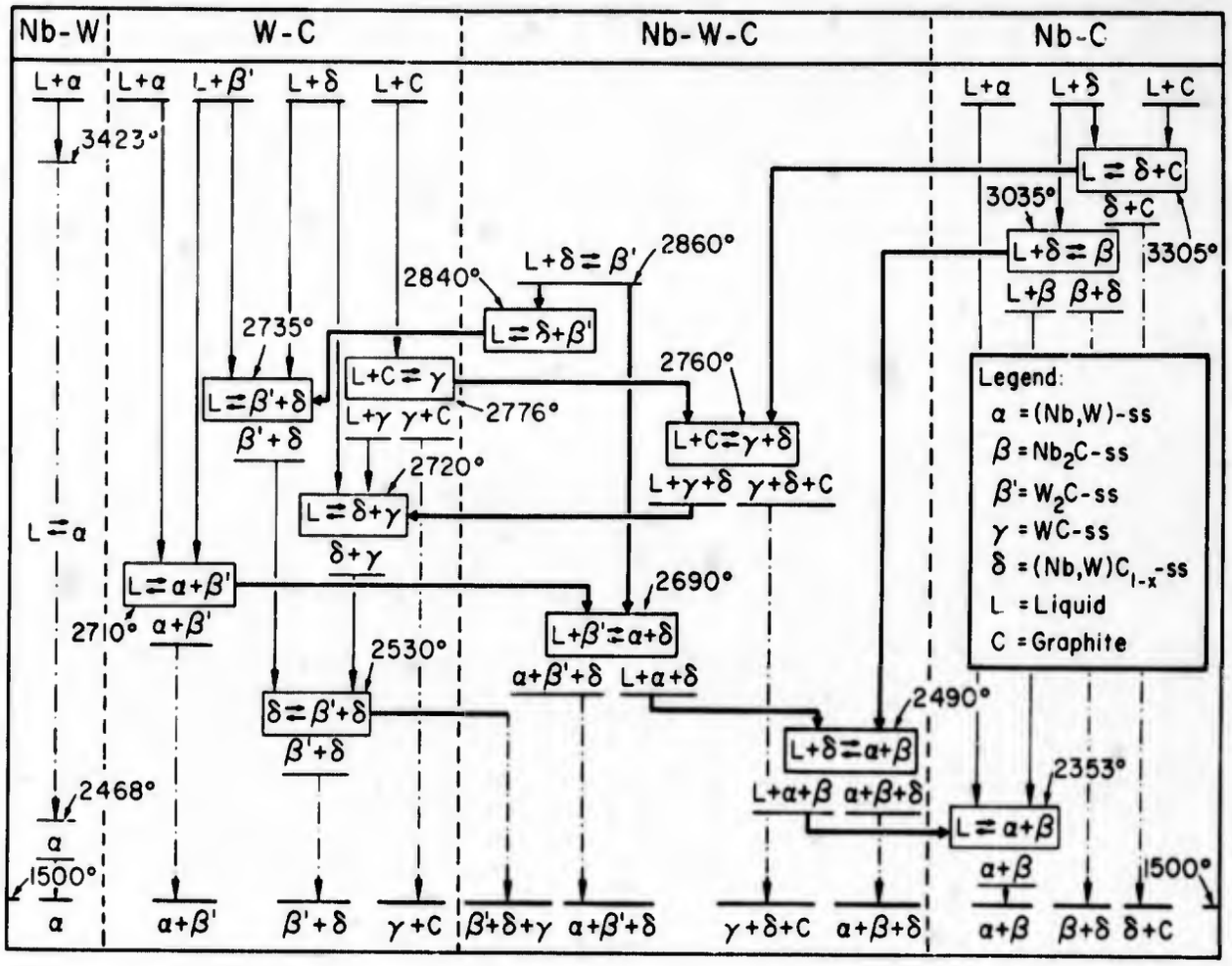

Figure 2. Reaction Diagram for the Nb-W-C System.

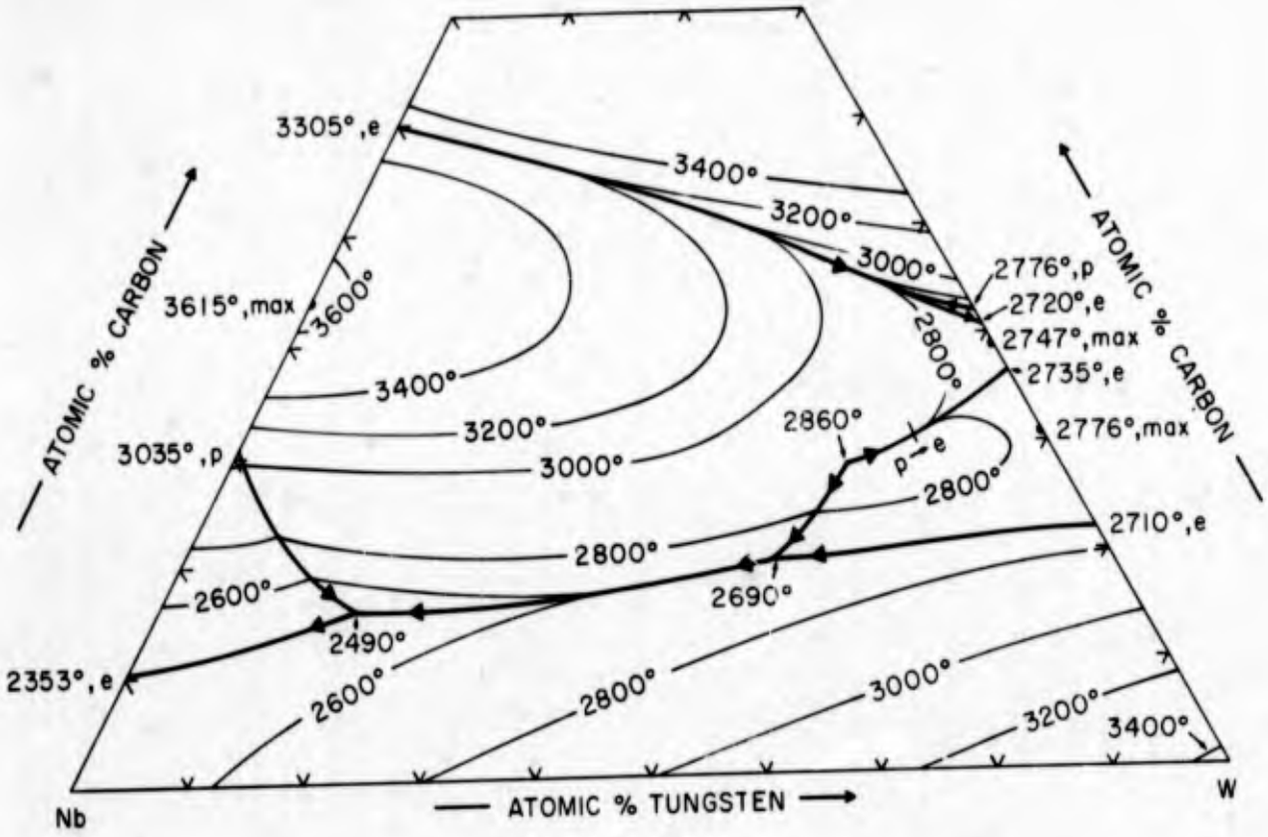

Figure 3. Liquidus Projections in the Nb-W-C System

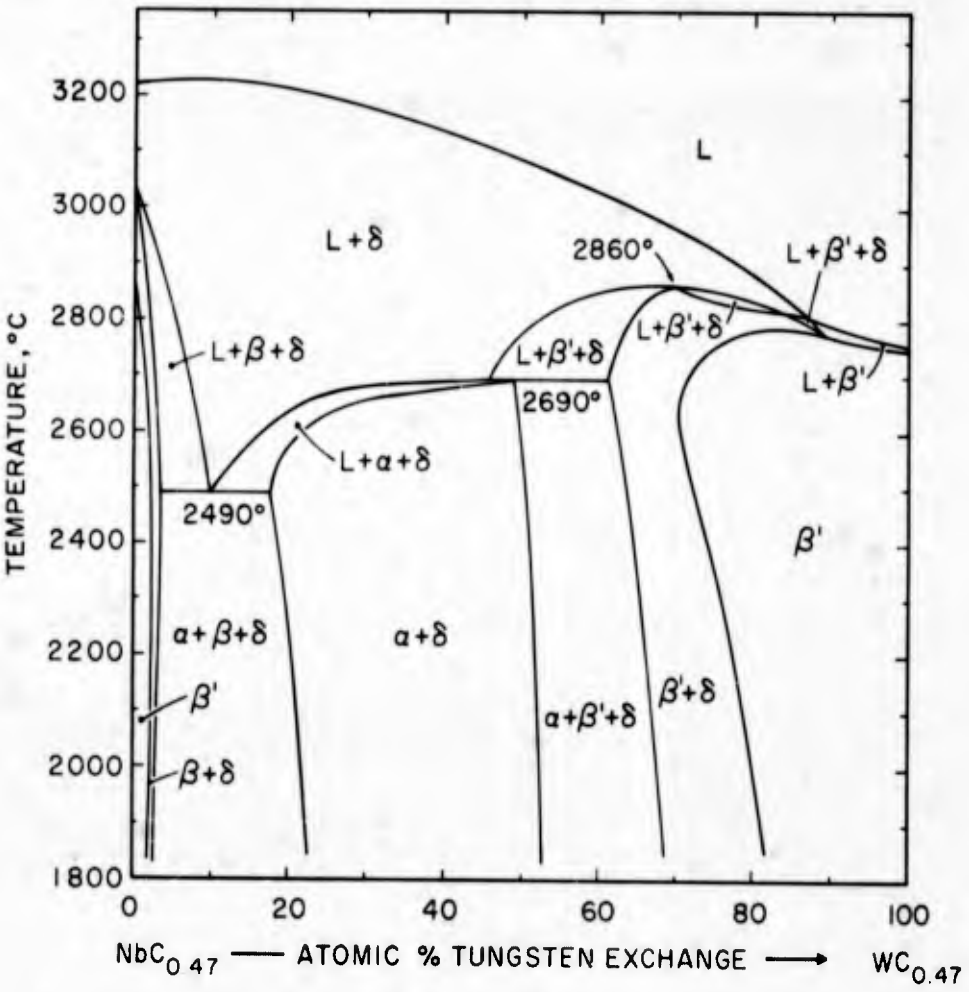

Figure 4. Isopleth at $NbC_{0.47}$-$WC_{0.47}$.
(Transitions in Nb_2C and W_2C not taken into account).

II. LITERATURE REVIEW

In the boundary systems, niobium and tungsten are known to form a continuous series of solid solutions[10-14]. The investigations of the niobium-carbon system by E.K. Storms and N.H. Krikorian[15] and H. Kimura and Y.Sasaki[16] were recentlv supplemented by E. Rudy et al.[17, 18]. The system, Figure 5, contains a very refractory monocarbide with the B1-structure (Table 1) and a subcarbide, which exists in at least two different states of sub-lattice order at low temperatures[17-23], and a disordered state above approximately 2500°C[17, 18]. The melting point measurements by E. Rudy et al.[17] are in close confirmation of the data by H. Kimura and Y.Sasaki[16].

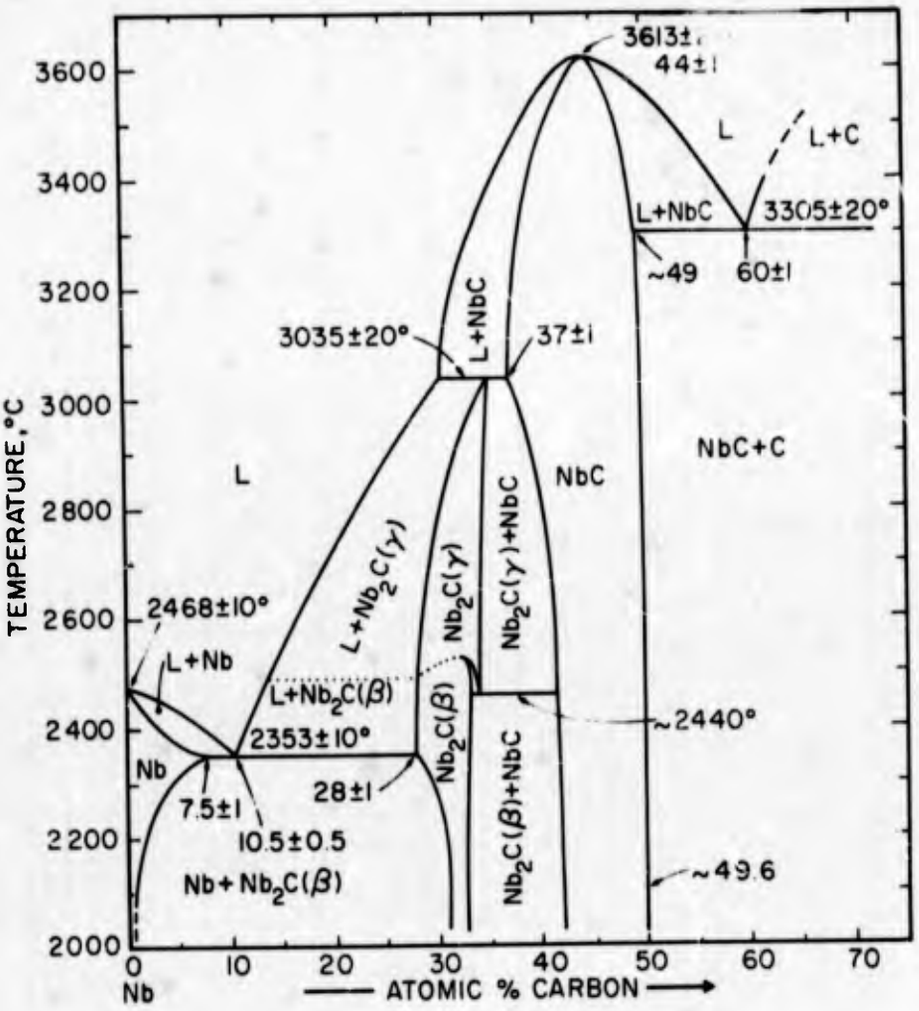

Figure 5. Phase Diagram of the Niobium-Carbon System.

Table 1. Structure and Lattice Parameters of Niobium and Tungsten Carbides

Phase	Structure	Lattice Parameters, Ångstrom
Nb_2C	1. T < 1200°C Orthorh.	a=12.36 Å, b = 10.85 Å, c= 4.968 Å (18,23)(*) a=10.92 Å, b=4.974 Å, c=3.090 Å (22)(**)
	2. 1200-2500°C Probably hex. -Fe_2N-type	a=5.40 Å, c=4.960 Å (19)(***)
	3. T>2500°C Hex.approach. L'3-type	a=3.125 Å c=4.972 Å at 33.3 At.% C (15)
NbC	fcc., B1-type	a=4.431 at 41.5 At.% C a=4.470 at ~50 At.% C (19)
W_2C	hex., L'3-type hex., C6-type(31)	a=2.992 Å c=4.722 Å (30)
		a=2.985 Å c=4.716 Å at 29.5 At.% C (24)
		a=3.000 Å c=4.730 Å at 32.8 At.% C
	2100° to 2480°C: orthorh., D_{2h}^{14}-Pb	a=4.728 Å b=6.009 Å c=5.193 Å at 32.6 At.% C (28) (+)
α-WC_{1-x}	fcc., B1-type	a=4.23 Å (32) a=4.215 Å (26, 27) a=4.22$_0$ Å (24)
WC	hex., D_{3h}^1-P6m2	a=2.900 c=2.831 (30) a=2.8063 c=2.8386 (33)

* The orthorhombic axes are related to the (distorted) hexagonal subcell by: $a_{o.r.} \sim 4a_{hex}$; $b_{o.r.} \sim 2a_{hex}\sqrt{3}$; $c_o = c_{hex}$.

** $a_{o.r.} \simeq 2a_{hex}\sqrt{3}$; $b_{o.r.}$ c_{hex}; $c_{o.r.} \simeq a_{hex}$.

*** $a = a_{hex.\,subcell}\sqrt{3}$; $c = c_{subcell}$

\+ $a_{o.r.} = c_{hex}$; $b_{o.r.} \simeq 2a_{hex}$; $c_{o.r.} \simeq a_{hex}\sqrt{3}$

The rather complex phase relationships in the tungsten-carbon system were clarified in detail only recently[24, 25], after the gross features of the system had been established previously by the work of R.T. Doloff and R.V. Sara[26, 27]. The system contains three intermediate phases, W_2C, WC, and α-WC_{1-x} (Table 1), of which α-WC_{1-x} is stable at high temperatures only[26, 27], and W_2C exists in at least two different states of sublattice order[28]. The mode of transformation is dependent upon the stoichiometry: Hyperstoichiometric compositions cannot exist in the ordered state; upon cooling through a critical temperature range, the stoichiometric carbide separates into two phases, an understoichiometric alloy which is ordered, and a hyperstoichiometric alloy which is disordered and decomposes at 2380°C into the ordered modification and tungsten monocarbide. No evidence was found for a two-phased transformation process in the substoichiometric carbide.

Previous investigations on ternary Nb-W-C alloys include the establishment of extended solubility along the section NbC-WC[9, 34, 35] and of a melting point minimum along the same section by C.Agte and H.Alterthun[36]. More recently, a temperature section of the system at 1700°C was established by E. Rudy and F. Benesovsky [work quoted in (4)] and a cursory examination of the equilibria at 2500°C was undertaken by A. Taylor and N.J. Doyle[37].

III. EXPERIMENTAL

A. STARTING MATERIALS AND ALLOY PREPARATION

The elemental powders as well as specially prepared carbide master alloys consisting of Nb_2C, NbC, W_2C, and WC served as starting materials for the preparation of the experimental alloys.

The impurities in the niobium powder (Wah Chang Corporation, Albany, Oregon; overall purity better than 99.8%) were as follows (in ppm): O-<420; N-<90; C-30; Ta-400; Zr-200; and the sum of other metallic impurities-<400. A lattice parameter of $a = 3.306$ Å, obtained from an exposure with Cu-K_α radiation, is consistent with lattice spacings given in the literature[14c].

The major contaminants in the tungsten powder (Wah Chang Corporation, Albany, Oregon) in ppm, were: Mo-70; O-290; Fe-60; Ni-20; N-400, sum of other metallic impurities-<100. The lattice parameter was $a = 3.165_1$ Å.

The spectrographic grade graphite powder was purchased from the Carbon Products Division of Union Carbide. It contained less than 2 ppm impurities.

The carbides were prepared by reacting the cold-compacted mixtures of the elemental powders in a graphite-element furnace under vacuum (Nb_2C, W_2C), or under hydrogen (WC, NbC). The reaction conditions were 2 hrs at 1850°C for W_2C and Nb_2C, and 4 hrs between 2000 and 2100°C for NbC and WC. After cooling under vacuum, the reaction lumps were comminuted to a grain size of less than 60 microns in carbide-lined ball mills. Cobalt traces picked up during milling were removed by acid-leaching in a mixture of hydrochloric and sulfuric acid, the resulting slurry centrifuged, washed with ether, and then vacuum dried. Until they were used, the powders were stored under helium in hermetically sealed plastic jars. The carbon analyses of the carbon powders are listed in Table 2. Oxygen analyses indicated contamination levels below 150 ppm for any of the carbide master alloys.

Table 2. Carbon Analyses and X-ray Data on Carbide Starting Materials.

Carbide	Carbon Content, At%	Phases Present	Lattice Parameters, Å
Nb_2C	33.2 ± 0.2	Nb_2C + trace monocarbide	a=3.124; c=4.963
NbC	49.2 ± 0.2	NbC	4.470
W_2C	32.5 ± 0.3	W_2C	a=2.998; c=4.730
WC	50.7 ± 0.3	WC	a=2.906; c=2.837

Alloys from the binary Nb-W system were cold-pressed and sintered for 4 hrs at 1650°C under a vacuum of better than 4×10^{-6} Torr. Ternary alloys from the concentration range Me + Me_2C were also cold-pressed and then pre-homogenized under vacuum, while carbon-richer samples were prepared by hot-pressing in graphite dies. The surface reaction zones of the hot-pressed specimens were removed by grinding and then the samples subjected to the same homogenization treatments as the cold-pressed mixtures.

All in all, close to 300 specimens were prepared. Approximately 30 were used for DTA-studies, 100 for the determination of the solidus envelope of the system, and the remainder for the investigation of the solid state sections of the system and for the study of the temperature variation of selected equilibria.

Homogenization treatments were carried out in a tungsten-mesh element furnace manufactured by the R. Brew Company. Major equilibration treatments for the determination of the solid equilibria were 87 hrs at 1500°C, and 70 hrs at 1700°C (both under a vacuum of better than 4×10^{-6} Torr; 6 hrs at 2200°C, and 2 hrs at 2500°C, both under 1.1 atmospheres helium.

Additional treatments, mostly in the solidus + liquidus region, were carried out in the DTA- and the melting point furnace and the specimen quenched in tin where it proved necessary.

B. DETERMINATION OF MELTING TEMPERATURES AND DIFFERENTIAL-THERMOANALYTICAL STUDIES

Melting temperatures were measured using the method devised by M. Pirani and H. Alterthum[38]. The apparatus and the operating procedures used in this laboratory have been amply described in previous publications[39] and need therefore not be repeated in detail here.

In carrying out the measurements, the specimens were first heated under vacuum until no further degassing was noticeable. This usually occurred after a 2 to 3 minute treatment at temperatures between 2000 and

2400°C. The furnace chamber was then filled with high purity helium to pressures varying between 1.1 atmospheres for metal-rich alloys, and 2.5 atmospheres for samples located in the monocarbide region. These higher gas pressures for high melting specimens proved to be necessary in order to cut the carbon loss rates due to vaporization.

The differential thermoanalytical studies[40] were also carried out under high purity helium, after the sample had received a brief degassing treatment at temperatures between 1800 and 2200°C. Annealed and high temperature-degassed graphite served in all cases as container material and also as comparison standard. Analogous to the observations on Nb-Mo-C alloys[2], the interaction of Nb-W-C alloys with graphite also occurs rather preferential with respect to niobium and thus the DTA-measurements on metal-rich (<40 At.% C) alloys could be extended to fairly high temperatures without deleterious interference from the container. After the runs, all DTA-specimens were sectioned, microscopically inspected, and also analyzed by X-ray diffraction.

C. METALLOGRAPHIC, X-RAY, AND CHEMICAL ANALYSIS

Metallographic preparations were made from approximately one-half of the experimental alloy material which included sintered, melted, and annealed DTA and melting point specimens. The specimens were mounted in a mixture of diallyl-phtalate and lucite-coated copper powder and preground on silicon carbide papers. The coarse ground specimens were polished on microcloth using a slurry of Linde "B" alumina (0.05 μ) in 5% chromic acid solution. The etching procedures, Table 3, varied with the composition of the alloys.

Carbon in the alloys was determined in the well-known manner by combustion and subsequent conductometric analysis of the gas mixture. For the determination of elemental graphite in the specimens, the powdered samples were first dissolved in a mixture of nitric and hydrofluoric acid, the graphite residue filtered off, washed thoroughly with methanol and warm heptane, and then run in the combustion apparatus.

Table 3. Etching Procedures for Nb-W-C Alloys

Alloys from the Composition Area	Etching Procedure
$Nb-W-W_{0.75}C_{0.25}-Nb_{0.75}C_{0.25}$	Electroetched in 0.5% oxalic acid solution
$Nb_{0.75}C_{0.25}-W_{0.75}C_{0.25}-W_{0.46}C_{0.54}-Nb_{0.46}C_{0.54}$ (**)	Swab-etched in 20% Murakami's solution (*)
$Nb_{0.46}C_{0.54}-C-W_{0.46}C_{0.54}$	Examined in the as-polished state

(*) Murakami's solution: 9.8 parts $K_3[Fe(CN)_6]$
0.2 parts KOH
90 parts H_2O

(**) Alloys located close to the Nb-C binary were etched in three steps: (a) electroetching in 0.5% oxalic acid followed by (b) a treatment with a 10% aqueous acid solution (6 parts HNO_3, 4 parts HF). This treatment removed surface stains caused by the electroetch. Etching was completed in a third step by swab-etching with Murakami's reagent.

Fifteen specimens, on a random selection basis, were analyzed for oxygen and nitrogen using the gas-fusion technique, and a few specimens were examined spectrographically for changes in low-level metallic impurities present in the starting materials. No metal analyses were performed, i.e. it was assumed that the relative metal concentration remained unchanged during the experiments.

As a rule, it was found, that the analyzed carbon contents agreed within 1.5 atomic percent with the weighed-in compositions. Oxygen and nitrogen contamination of all processed samples examined was less than 150 ppm. In view of this low contamination level, the effect of these interstitial impurities upon the measured phase equilibria is judged to be negligible.

The crystal structures of all phases occurring in the system were known from previous work and therefore only powder patterns using Cu-K_α radiations were prepared. The film strips were measured on a Siemens-Kirem coincidence scale with micrometer attachment. All exposures were evaluated with respect to nature and lattice dimension of the phases present in the alloys. The lattice parameter technique also was used to determine the coexisting phase compositions within the two- and three-phase fields in the system.

IV. RESULTS

A. THE BINARY NIOBIUM-TUNGSTEN SYSTEM

Melting data on eight binary alloys, shown together with the measurements by V.S. Micheev[12] in Figure 6, indicate a smooth transition between the melting points of the pure metals. Our measurements of the lattice parameters of the solid solution (Figure 7) agree closely with data previously reported by H. Buckle[10].

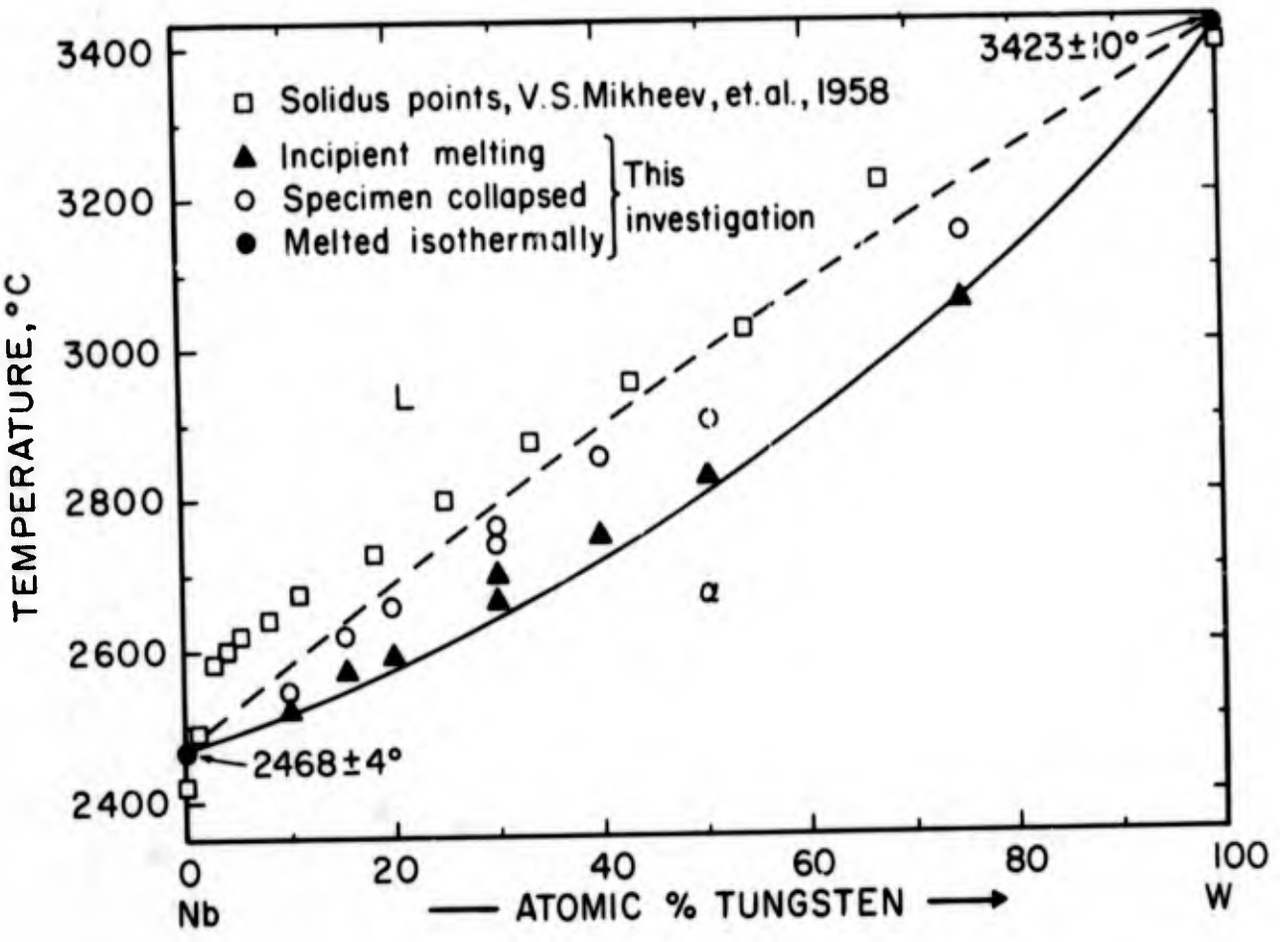

Figure 6. Melting Temperatures of Niobium-Tungsten Alloys.

(Temperature Figures Shown Refer to Mean Value and Reproducibility).

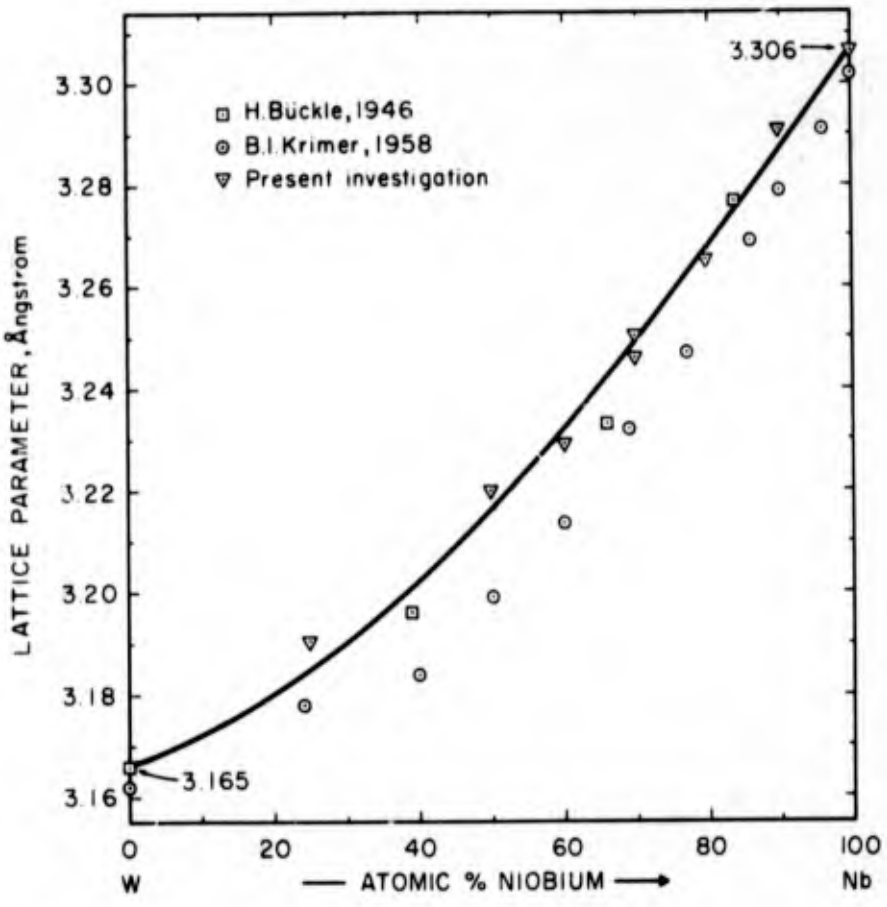

Figure 7. Lattice Parameters of the Nb-W Solid Solution.

B. THE TUNGSTEN-CARBON SYSTEM

Inasmuch as some of the finalized results, especially those concerning the mode of transformation of the subcarbide phase, were not contained in previous publications dealing with this system[24, 25], a brief account of them will be given now.

As a result of the new findings on the molybdenum-carbon system, which showed the phase separation reaction of the Me_2C phase to initiate only below a certain temperature, instead of forming a two-phase equilibrium up to melting temperatures as had been assumed at first[41], additional experiments were also performed in the tungsten-carbon system.

A large number of DTA-runs, carried out on specimens laid in small concentration intervals across the homogeneity range of the W_2C phase, revealed the existence of a number of thermal arrests.

The DTA-curves shown in Figure 8, are representative of data gained by multiple runs on each sample and the temperatures of the thermal arrests compiled in Figure 9 were independently verified by direct pyrometric readings in the black body holes of the specimens.

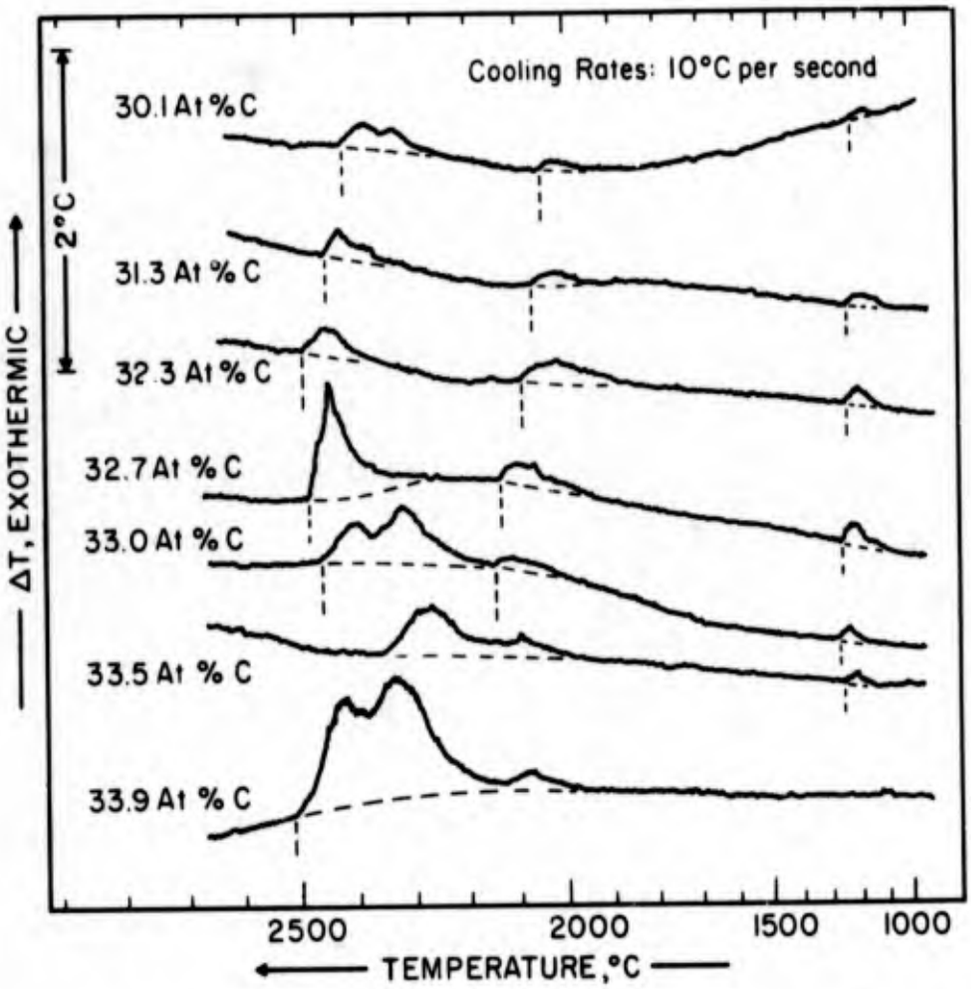

Figure 8. DTA-Thermograms (Cooling) of Alloys Located Within the Concentration Domain of the W_2C-Phase.

(Note: The small exotherm around 1250°C presumably is due to the incipient decomposition of W_2C).

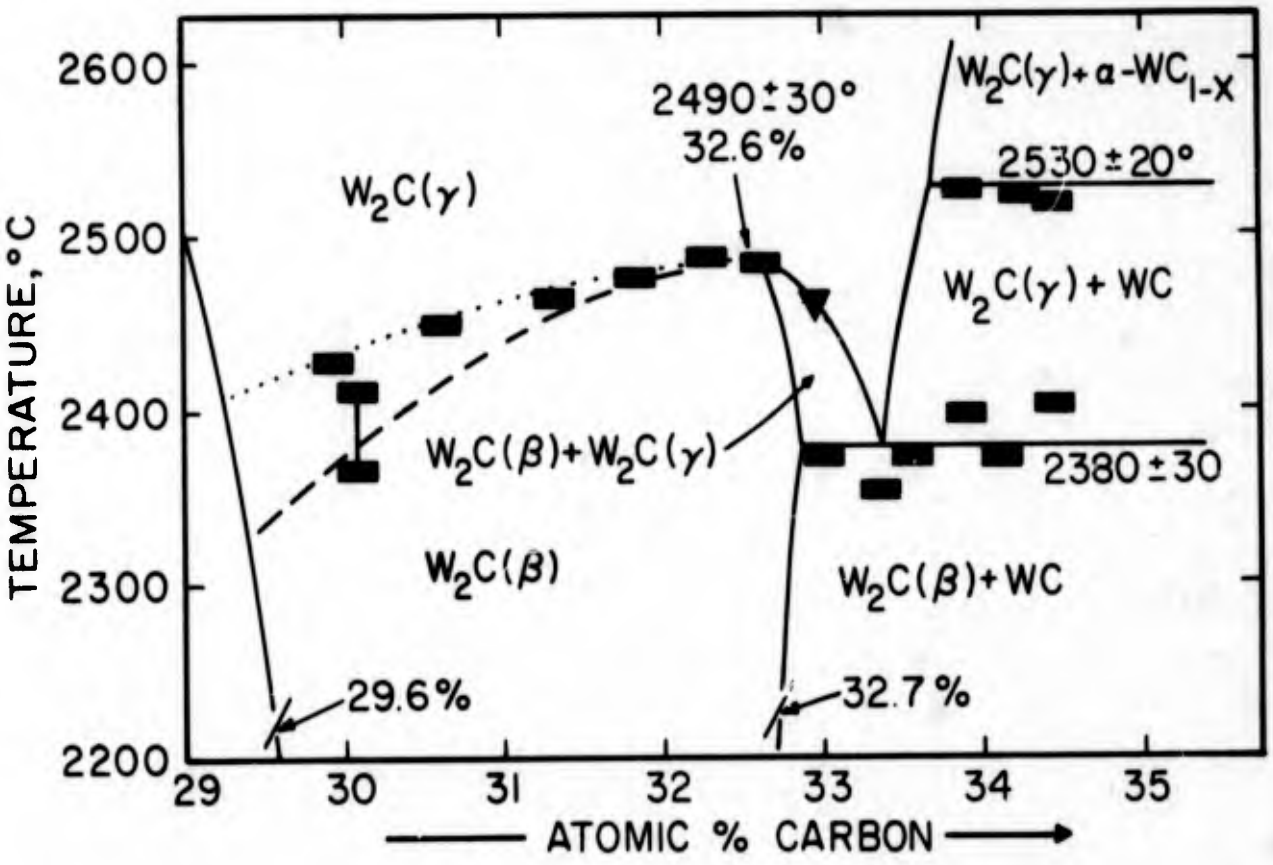

Figure 9. Summary of DTA-results Obtained on W_2C-Alloys.

These DTA-experiments, as well as X-ray diffraction studies on rapidly cooled (≤ 150°C/sec) alloys, indicated that both transitions, the one in the vicinity of 2500°C and the other at about 2100°C, proceeded with high speed. Although the similarities in the thermal arrests as well as the microstructures to the corresponding molybdenum carbide[24] is quite obvious, independent experimental evidence was sought to confirm this supposition. X-ray analysis of specimens quenched from the temperature range between 2100°C and 2500°C indeed yielded a pattern which could be interpreted[28] (Table 1) as being identical to the orthorhombically distorted, ordered modification of Mo_2C. On the other hand, the X-ray patterns of slowly cooled specimens, or of alloys which were quenched from temperatures below 2100°C, showed only the undistorted modification. Based on the X-ray evidence as well as the DTA-results one has to conclude, that the orthorhombically distorted modification

with an ordered structure analogous to that of Mo_2C undergoes a change-of-order transformation in the vicinity of 2100°C which probably is identical with the C6-type described by L.N. Butorina and Z.G. Pinsker[31]. It is worthwhile mentioning that storing the specimens for two or three days at room temperature appears to be sufficient to effect a transformation of the orthorhombic into the hexagonal or pseudohexagonal modification.

Further experimental data on the tungsten-carbon system are compiled in Figures 10, 11, and 12, and the finalized constitution diagram is depicted in Figure 13.

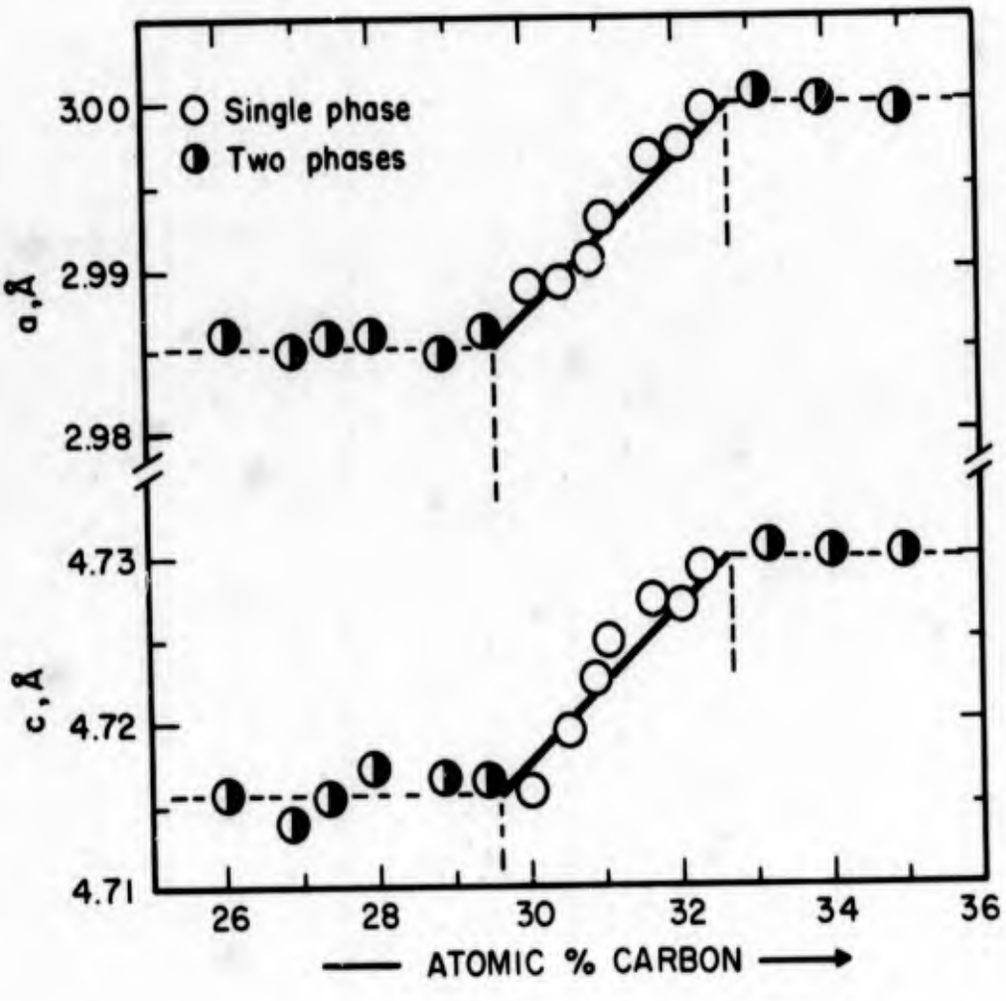

Figure 10. Lattice Parameters of W_2C.
(Alloys Rapidly Cooled from 2200°C).

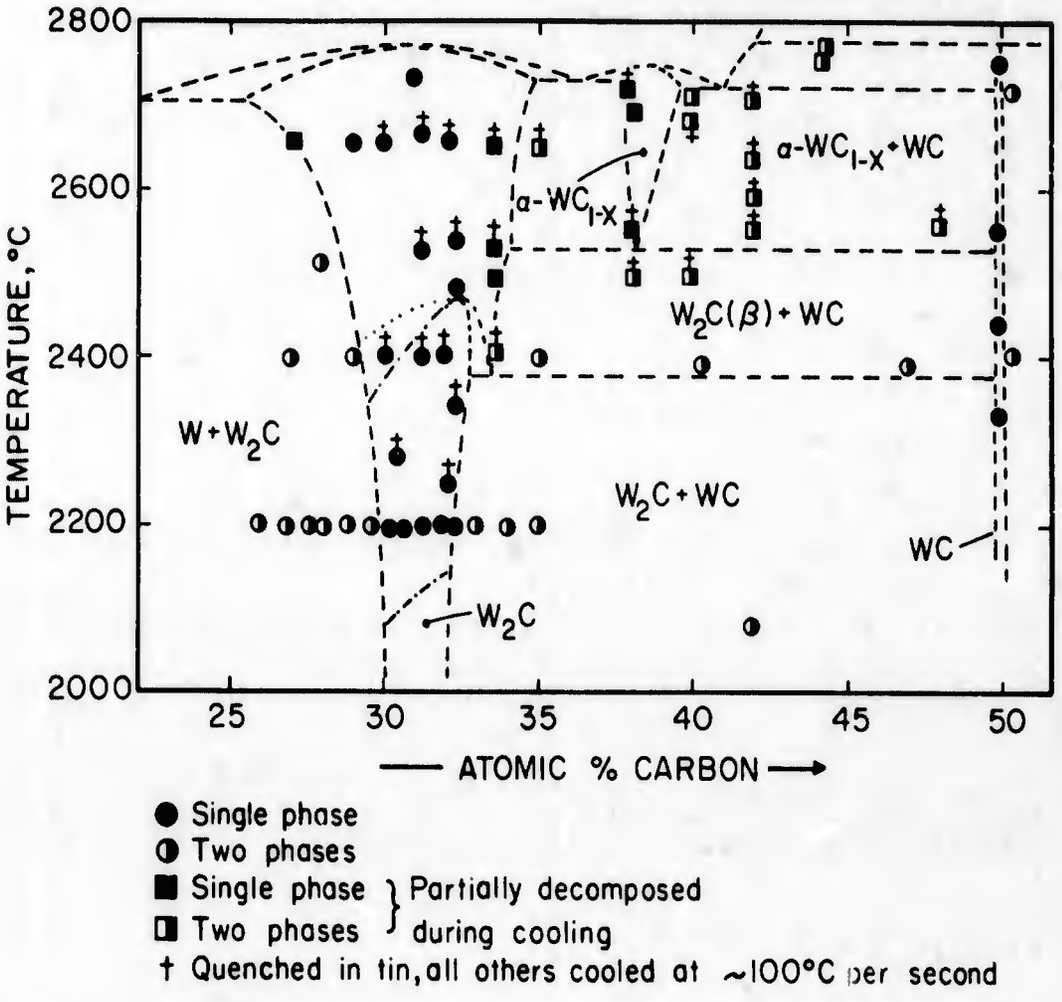

Figure 11. Qualitative Phase Evaluation of Heat-Treated and Quenched Tungsten-Carbon Alloys.

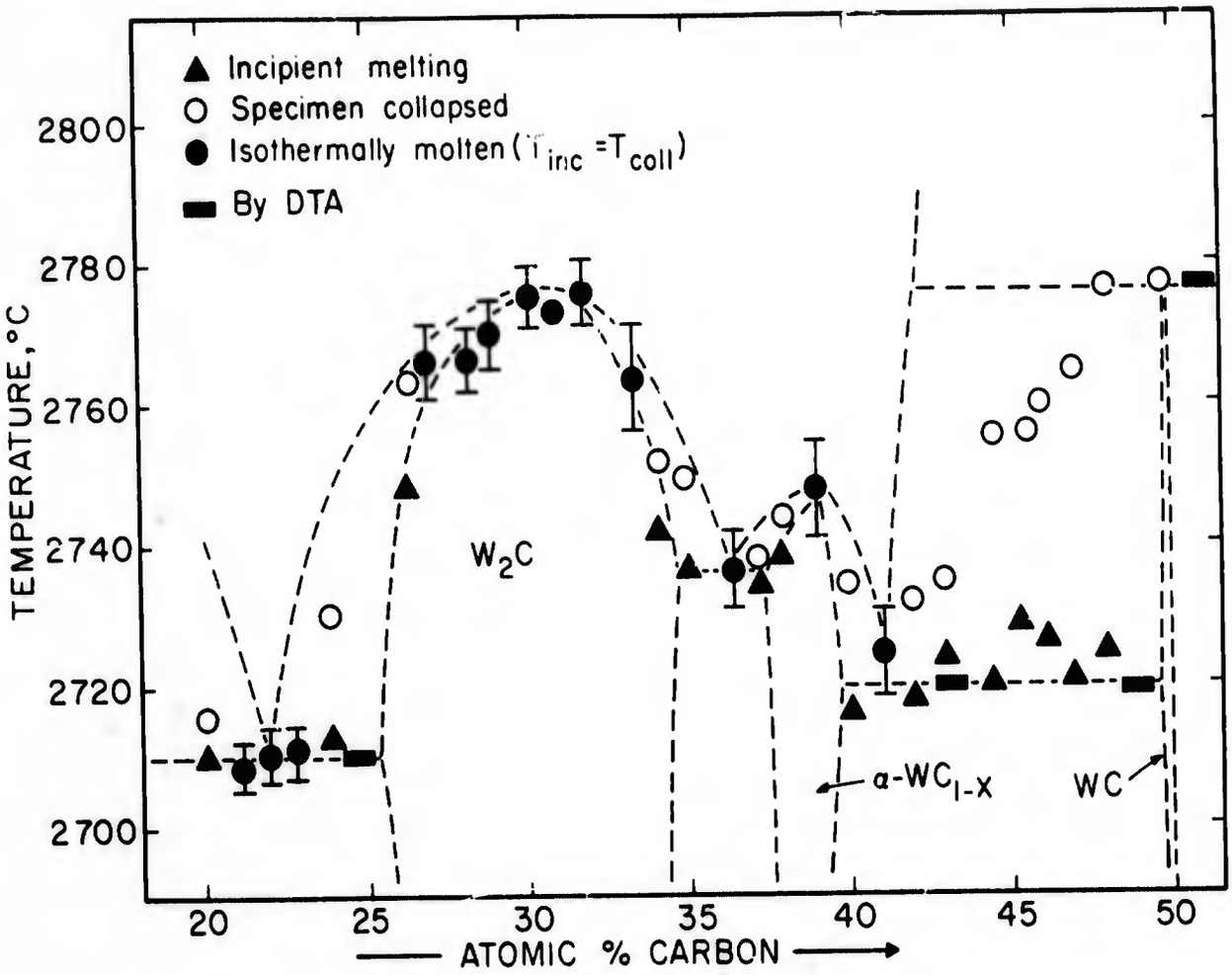

Figure 12. Melting Temperatures of Tungsten-Carbon Alloys.

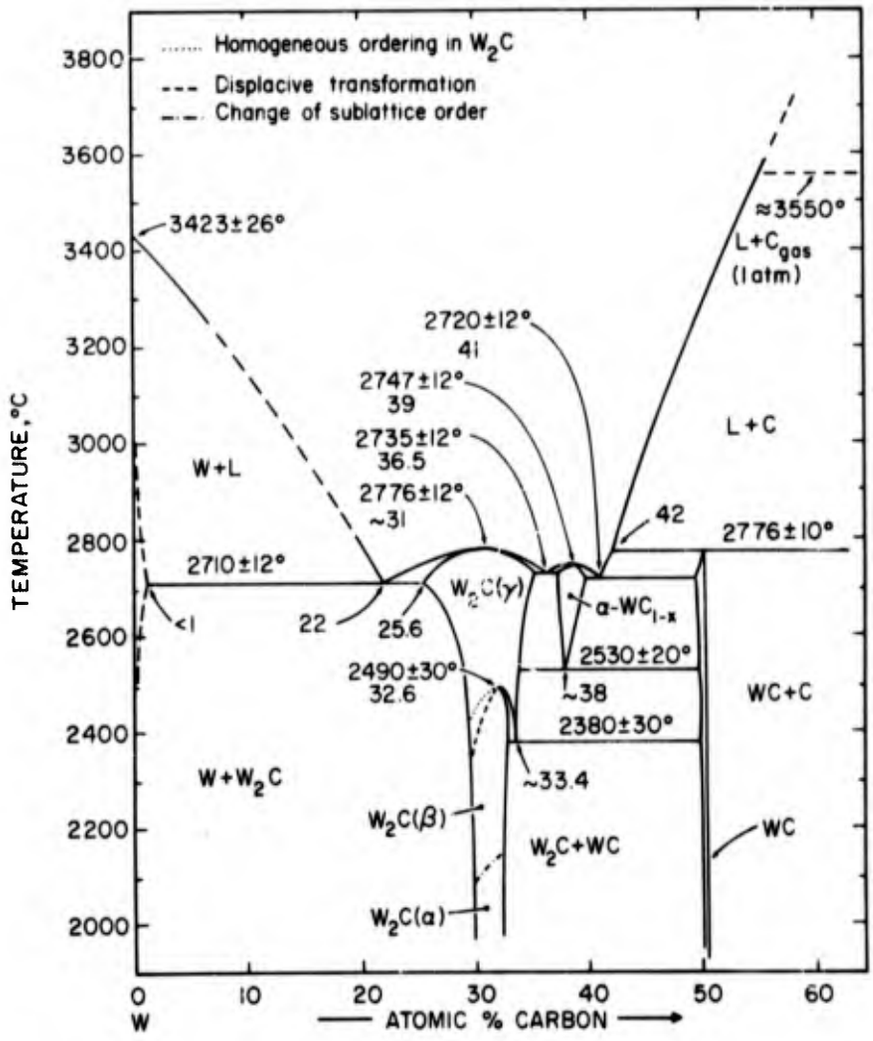

Figure 13. Finalized Constitution Diagram for the System Tungsten-Carbon.

(The Temperature Figures Refer to Mean Value and Estimated Overall Uncertainty).

C. THE NIOBIUM-TUNGSTEN-CARBON SYSTEM

1. Equilibria in the Solid State

The qualitative phase evaluation of the alloys equilibrated at 1700°C, Figure 14, confirms our previous finding[4] of an interrupted solid solution series of the subcarbides. At 1700°C, W_2C takes approximately 26 mole % Nb_2C into solid solution, increasing its parameters from a = 2.997 Å, c = 4.727 Å, for a slightly substoichiometric

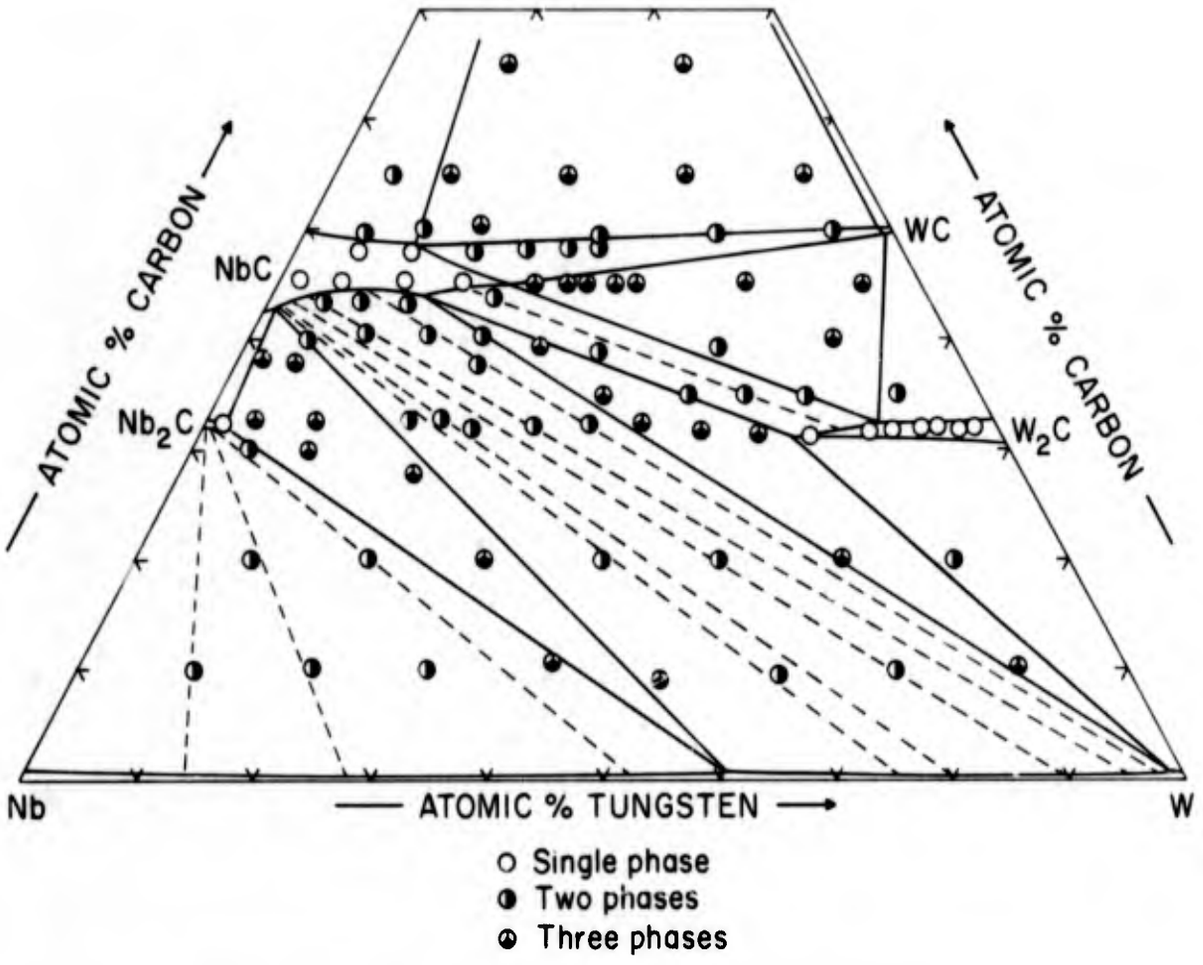

Figure 14. Sample Location and Qualitative Phase Evaluation of Nb-W-C Alloys Equilibrated at 1700°C.

The Tie Lines Indicated in the Two-Phase Field were Obtained From Lattice Parameter Measurements.

W_2C (Figure 15), to approximately a = 3.019 Å, c = 4.772 Å at the solubility limit. The tungsten exchange in Nb_2C was found to be small and alloys with more than approximately 5 mole % W_2C were three-phased, containing a mixture of metal, subcarbide, and monocarbide alloys. Lattice parameters, averaging a = 3.119 Å, c = 4.952 Å in three-phased alloys are only insignificantly different from the parameters of binary Nb-C alloys (a = 3.117 Å, c = 4.956 Å to a = 3.127 Å, c = 4.974 Å[17]) indicating that the solubilities indeed must be small.

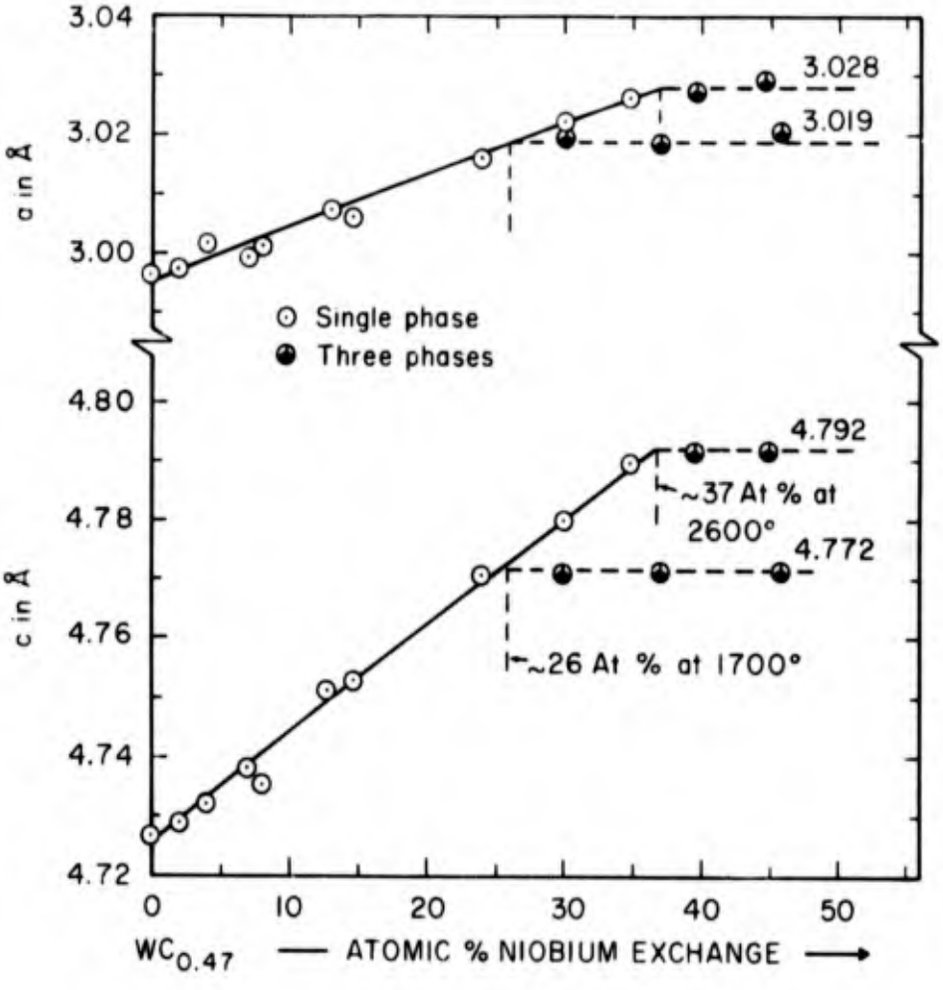

Figure 15. Lattice Parameters of the Tungsten-Rich Subcarbide Solid Solution.

(Parameters Based on Indexing According to the L'3-Type).

A maximum tungsten exchange of approximately 35 At.% in the monocarbide was derived from the evaluation of X-ray patterns (Figure 16).

The gross features of the phase relationships at 1500°C are identical to those found at 1700°C , only the mutual solubilities are somewhat lower.

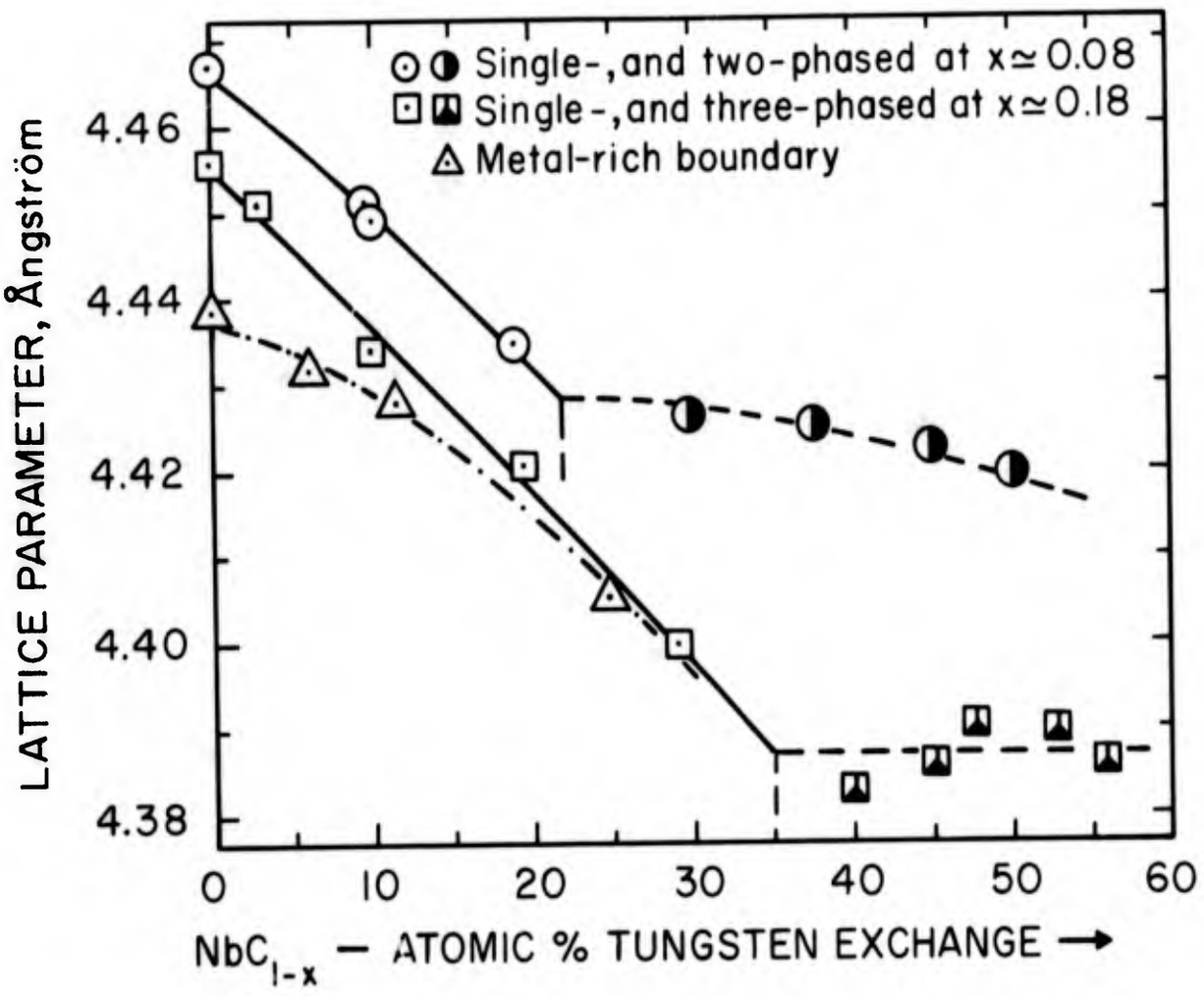

Figure 16. Lattice Parameters of the Cubic Monocarbide Solid Solution in 1700°C-Equilibrated Alloys.

The solubility in W_2C increases only slightly with increasing temperature (Figure 15), while the monocarbide phase extends to the Mo-C binary above 1960°C (Figure 17).

The decomposition of the substoichiometric monocarbide alloys with less than ~60 mole% WC_{1-x} is fairly slow and the alloys can be retained single-phased by ordinary furnace (radiation) cooling. For alloys located very near the tungsten-carbon binary, tin-quenching proved to be necessary to retain the cubic phase down to room temperature.

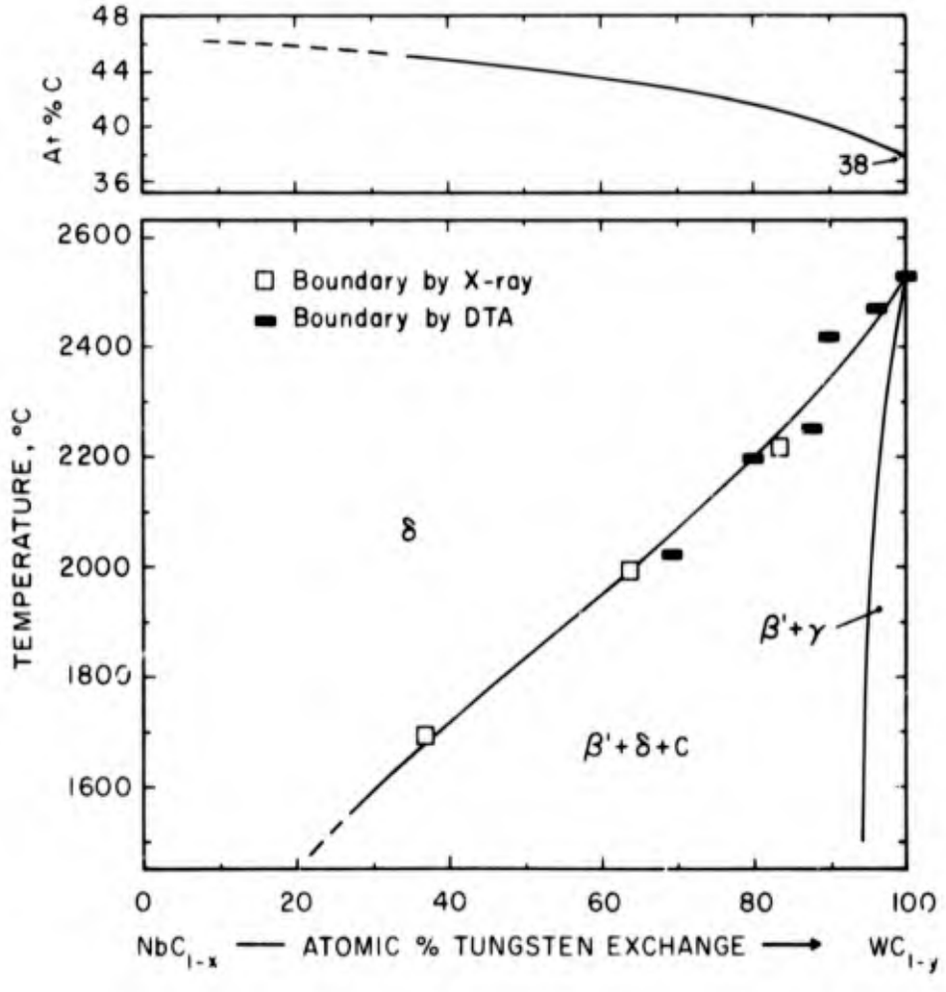

Figure 17. Maximum Tungsten Exchange in NbC.

Top: Concentration Line of the Vertex of the Three-Phase Equilibrium

$(Nb, W)C_{1-x}$ + $(Nb, W)_2C$ + WC-ss at the Monocarbide.

Typical DTA-data, showing the rapid decomposition of the tungsten-rich monocarbide alloys, as well as the lowering of the incipient decomposition temperature with increasing niobium content, are depicted in Figure 18. Additional lattice parameter data on the cubic monocarbide are presented in Figure 19.

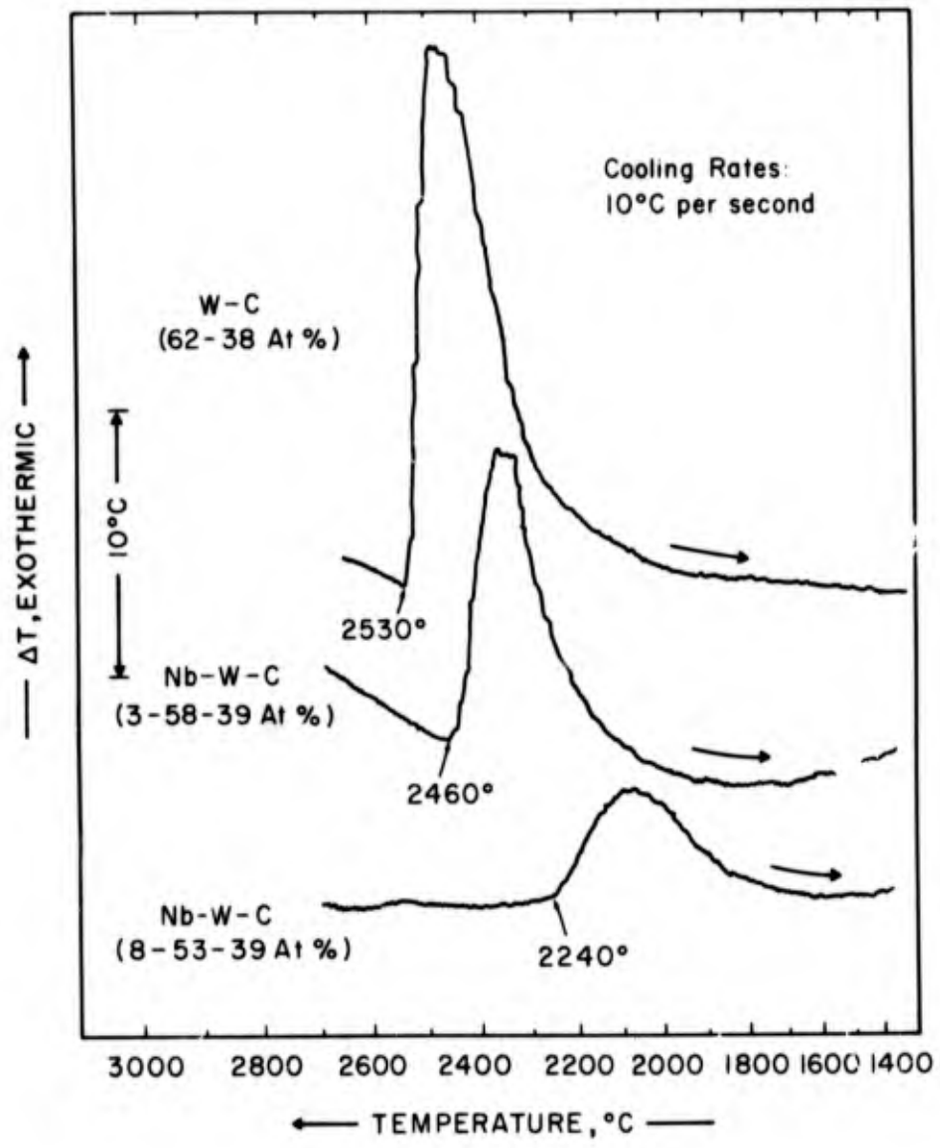

Figure 18. Disproportionation of the Cubic Phase in Binary Tungsten-Carbon (Top Curve) and Ternary Nb-W-C Alloys Located Near the Tungsten-Carbon Binary.

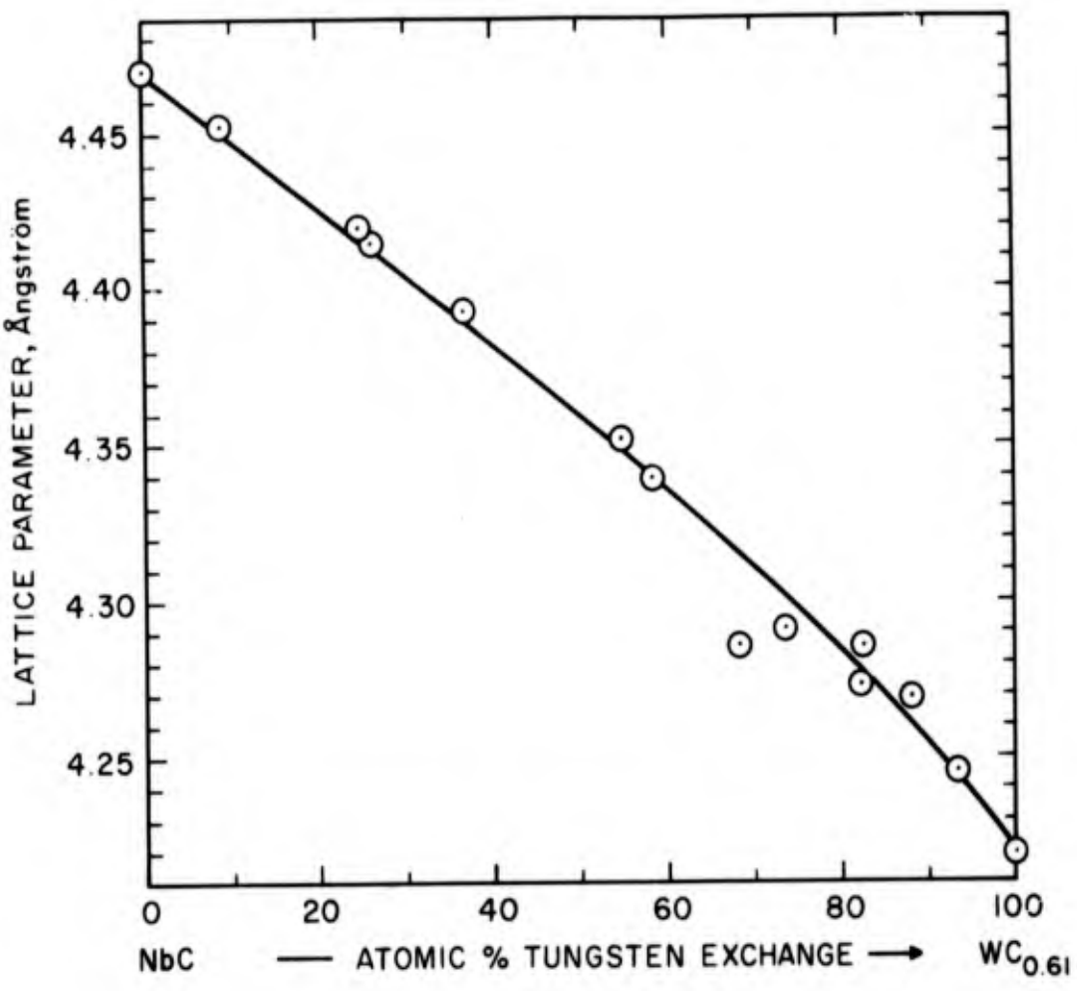

Figure 19. Lattice Parameters of the Cubic (B1) $(Nb, W)C_{1-x}$ Solid Solution Along the Section $NbC-WC_{0.61}$.

(Alloys with more than 10 At.% W Tin-Quenched From T > 2500°C).

In the alloy series equilibrated at 2500°C, Figure 20 the alloys located near the niobium corner of the system already contain liquid phase, and the two-phase area metal + monocarbide on the niobium-rich side is bounded by an equilibrium melt + metal and monocarbide phase. As to be expected from thermodynamic considerations, the swing of the tie lines in the two-phase field metal + monocarbide is much less pronounced at 2500°C than in the sections at 1500 and 1700°C.

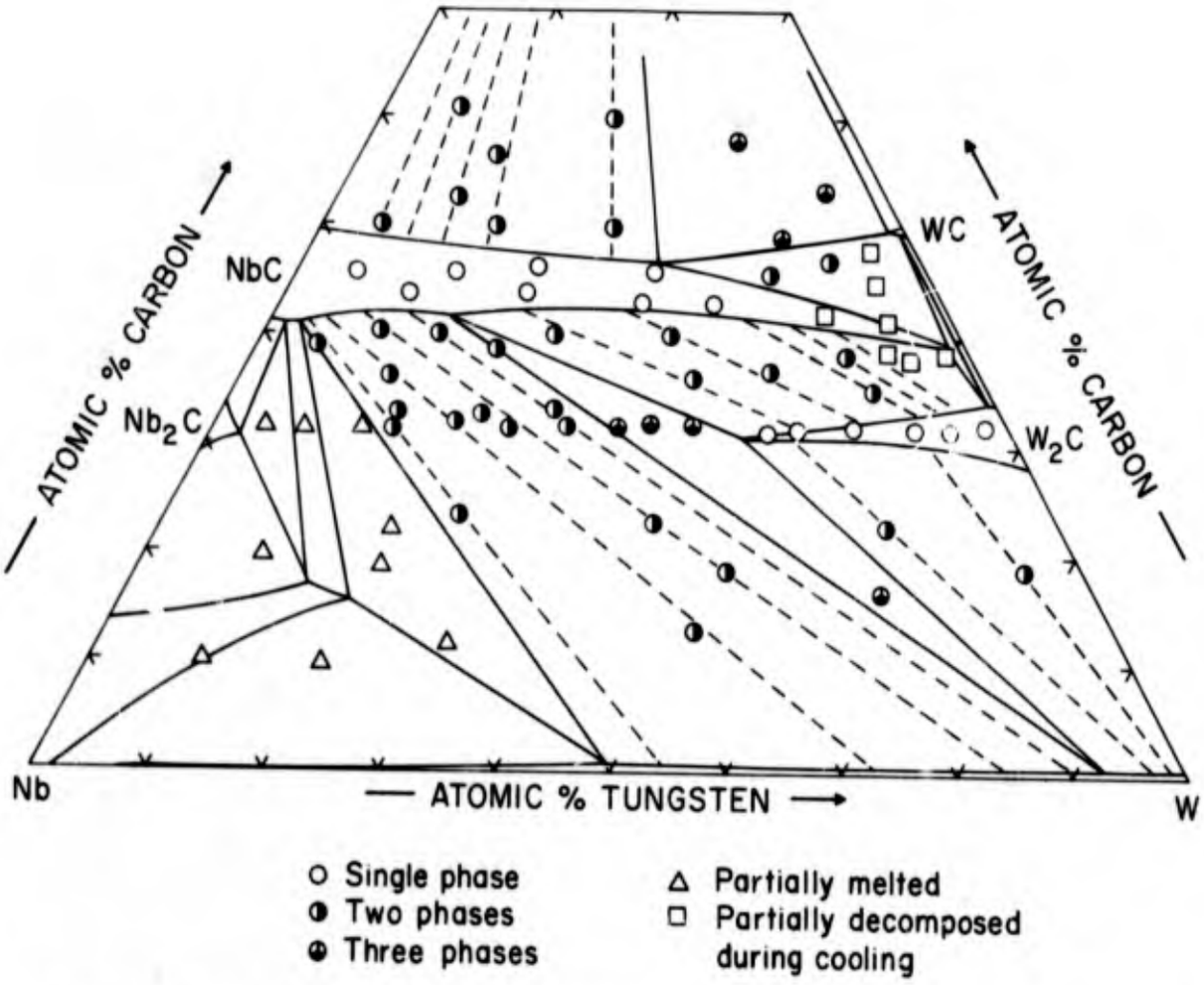

Figure 20. Qualitative Phase Evaluation of Nb-W-C Alloys Equilibrated at 2500°C.

2. Phase Equilibria in the Melting Range

With the exception of samples located very near the tungsten-carbon binary, which melted fairly sharp, melting in the alloys located along the metal-rich trough (Figure 21) was strongly two-phased. This heterogeneity in the melting behavior was still more pronounced in alloys located off to either side of the eutectic trough, and detection of incipient melting by the Pirani-technique became rather difficult.

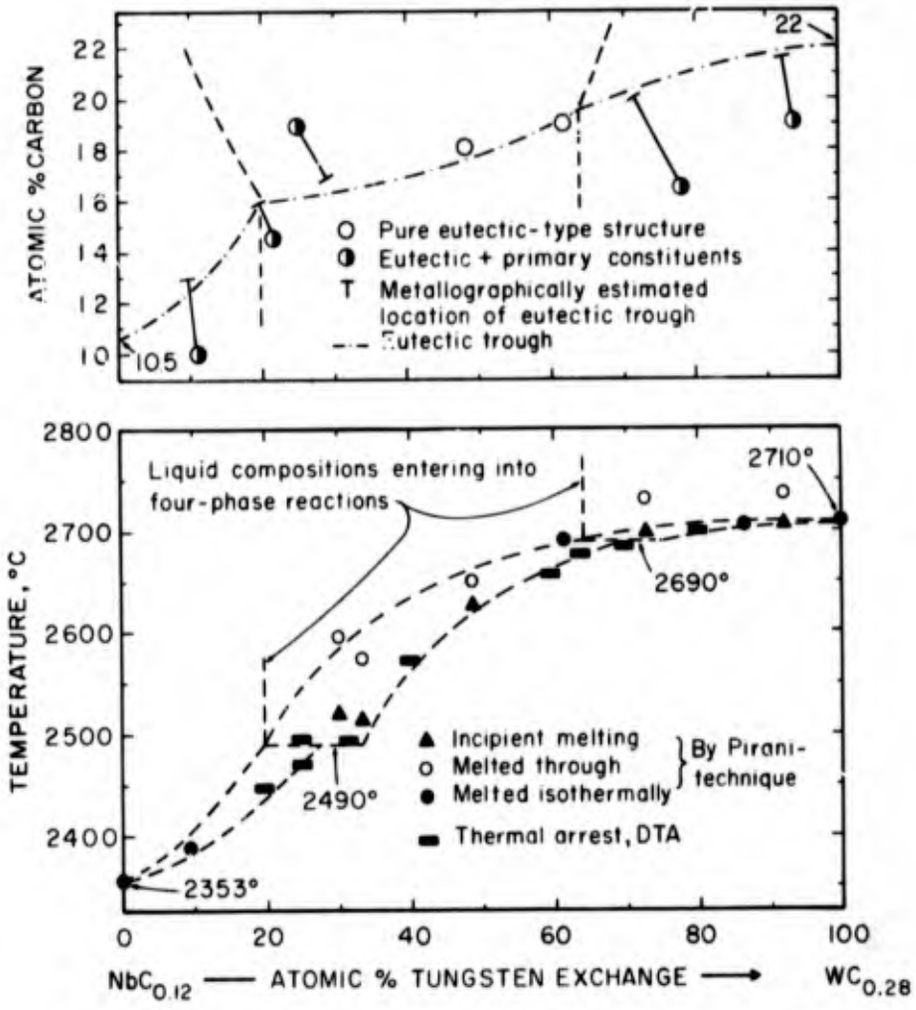

Figure 21. Melting Along the Metal-Rich Eutectic Trough in the Nb-W-C System.

The location of the eutectic trough near the niobium-molybdenum edge system was mainly delineated by microscopic inspection of melted and then rapidly cooled alloys (Figures 21, 22, 23, 24). Although solidification across the entire range of ternary compositions is bivariant, the appearance of the structure remains distinctly eutectic-like.

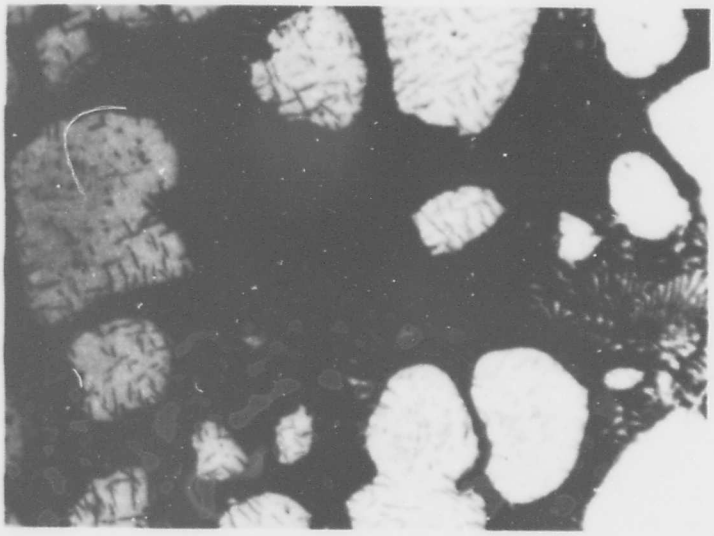

Figure 22. Nb-W-C (80-10-10 At.%) Melted and Rapidly Cooled. X1000
Primary Metal, with Intragranular Carbide Precipitates, in a Eutectic-Like Matrix Consisting of Metal and Nb_2C Phase.

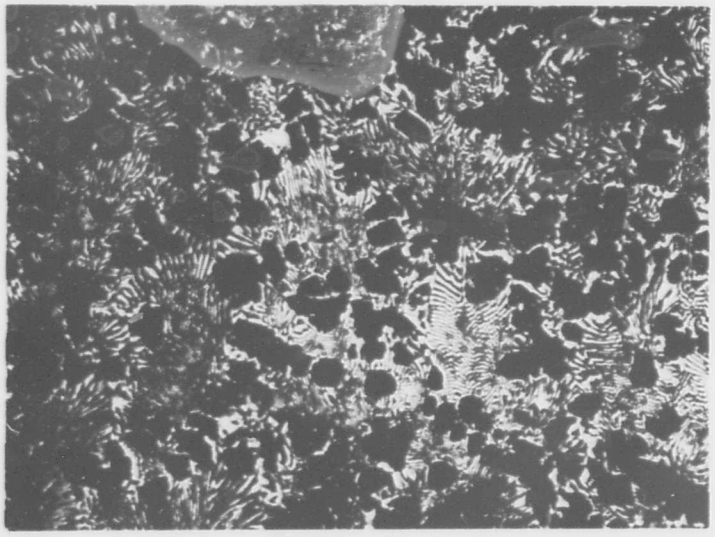

Figure 23. Nb-W-C (36-50-14 At.%), Melted and Rapidly Cooled. X375

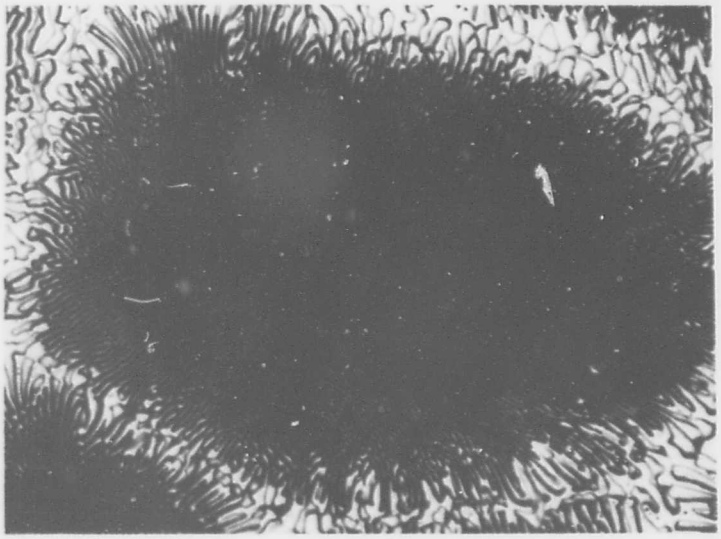

Figure 24. Nb-W-C (37-44-19 At.%), Melted and Rapidly Cooled. X 350

Eutectic Grain Showing the Bivariant Solidification Along the Metal-Monocarbide Eutectic Trough.

Specimens located on the section Nb_2C-W_2C melted extremely two-phased up to tungsten exchanges of approximately 80 At.%; at still higher tungsten contents the melting became increasingly sharp and metallographic inspection of as-melted alloys revealed single phase subcarbide alloys with only negligible coring. However, as evidenced by the melting behavior, as well as by metallographic and X-ray analysis of as-melted and of quenched alloys, a complete solid solution formation between the subcarbides does also not occur at high temperatures (Figures 25 through 29).

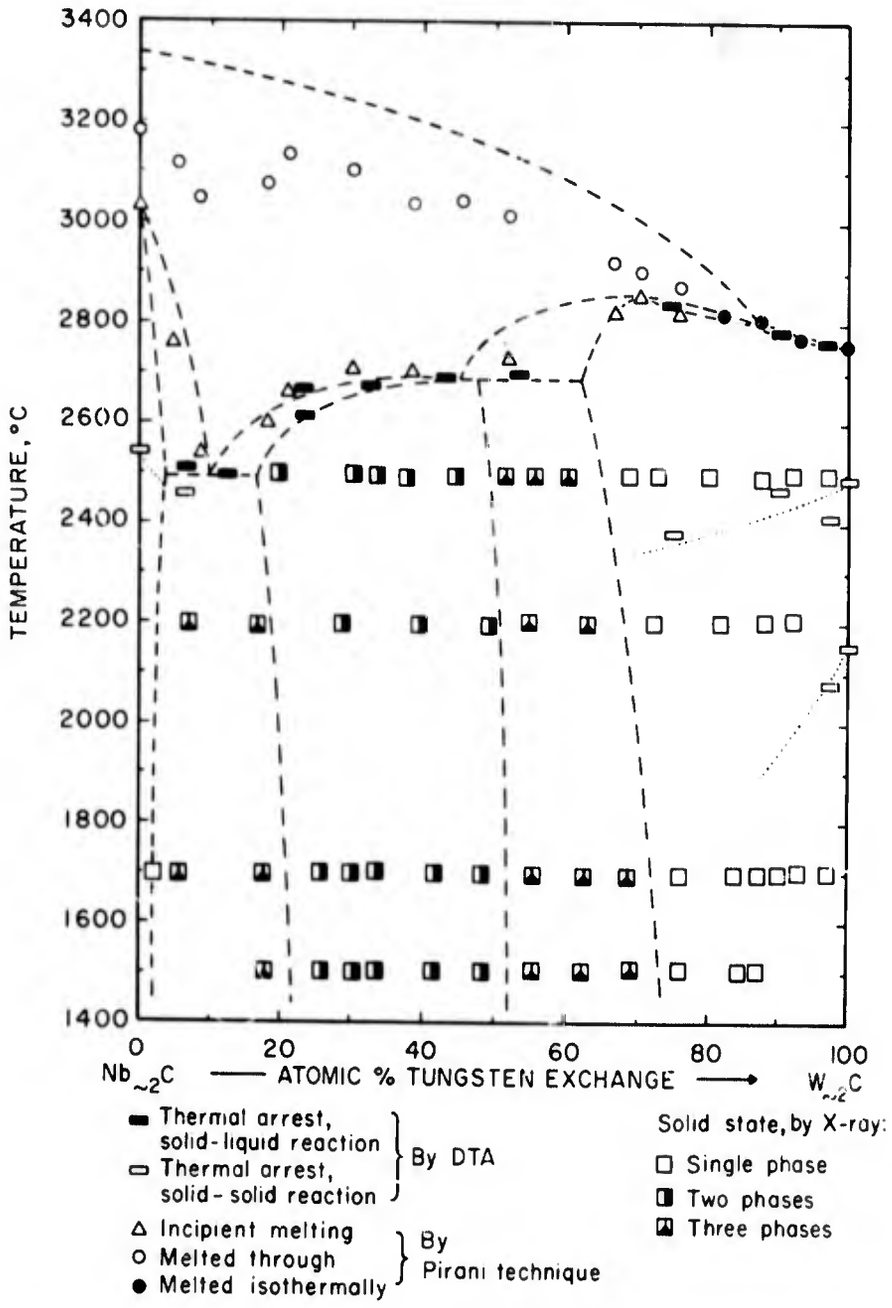

Figure 25. Melting and Qualitative Phase Evaluation of Alloys Located Along the Concentration Section Nb_2C-W_2C.

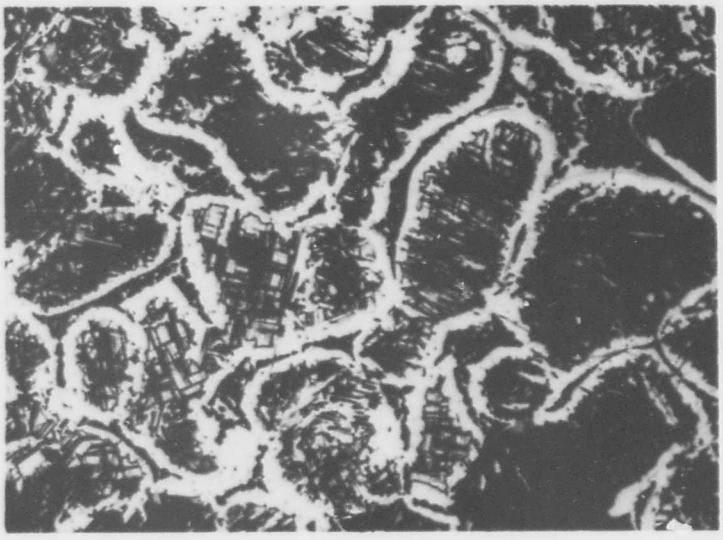

Figure 26. Nb-W-C (59-8-33 At.%), Cooled at ~15°C per Second from 3050°C. X320

Primary Monocarbide with Intragranular Subcarbide Precipitates, Secondary Subcarbide, Forming Walls Around the Monocarbide, and Rest Eutectic.

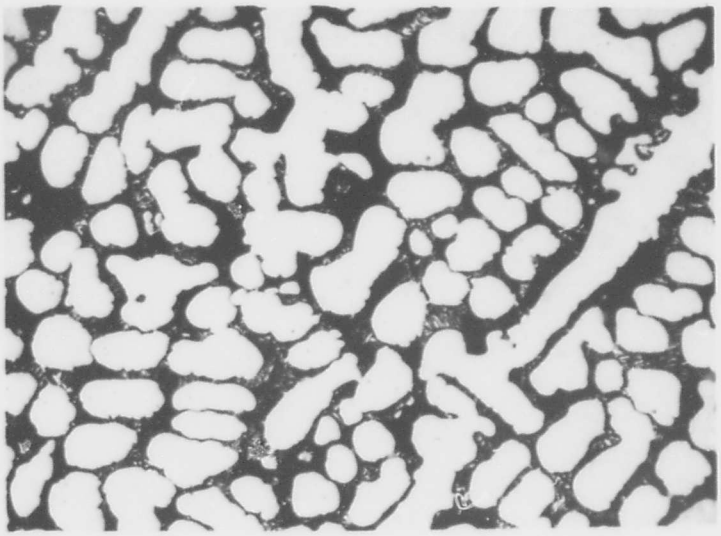

Figure 27. Nb-W-C (47-20-33 At.%), Rapidly Cooled from 3100°C. X500

Primary Monocarbide in Metal + Monocarbide Eutectic-Type Matrix.

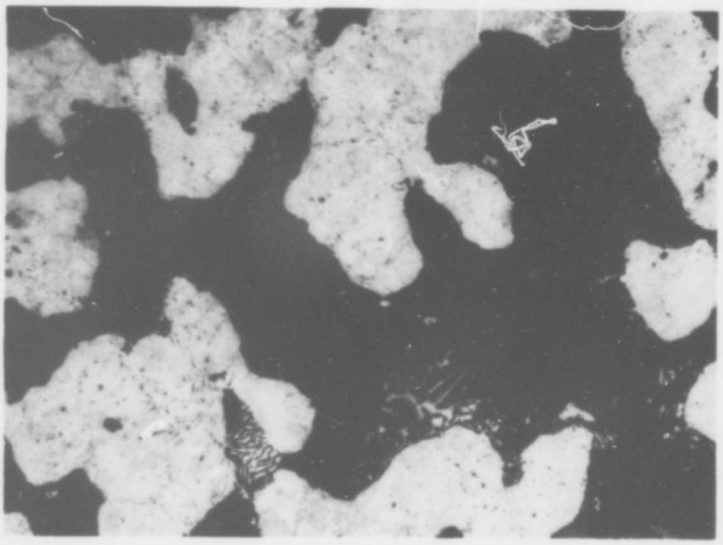

Figure 28. Nb-W-C (36-28-36 At.%), Rapidly Cooled from 3000°C. X520

Primary Monocarbide Grains, Surrounded by Small Amounts of Subcarbide, in a Eutectic-Type Matrix.

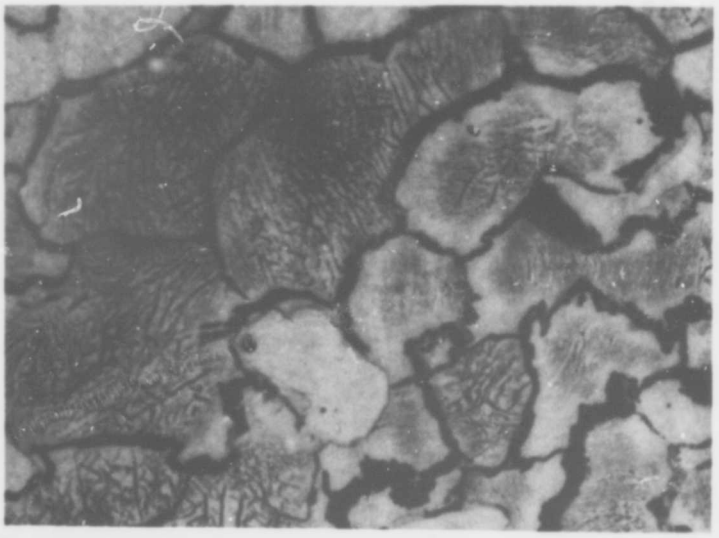

Figure 29. Nb-W-C (18-52-30 At.%), Cooled at ~150°C per Second From 2700°C. X600

Tungsten-Rich Subcarbide Phase with Intragranular Precipitates of Monocarbide and Metal Alloy, and Excess Metal Phase at Grain Boundaries.

The maximum solidus temperatures of the monocarbide phase vary smoothly between the congruent melting points of the binary compounds at 3615° and 2747°C, respectively. Since, in the ternary, the solidus temperatures are a function of the relative metal as well as the carbon content, it is necessary to investigate the entire solidus envelope in order to conclusively establish the melting behavior. From these data then, the temperatures as well as the composition of the maximum solidus can be derived. As an example, the datum points in Figure 30 were extracted from measurements on over 40 samples located within the homogeneity range of the monocarbide.

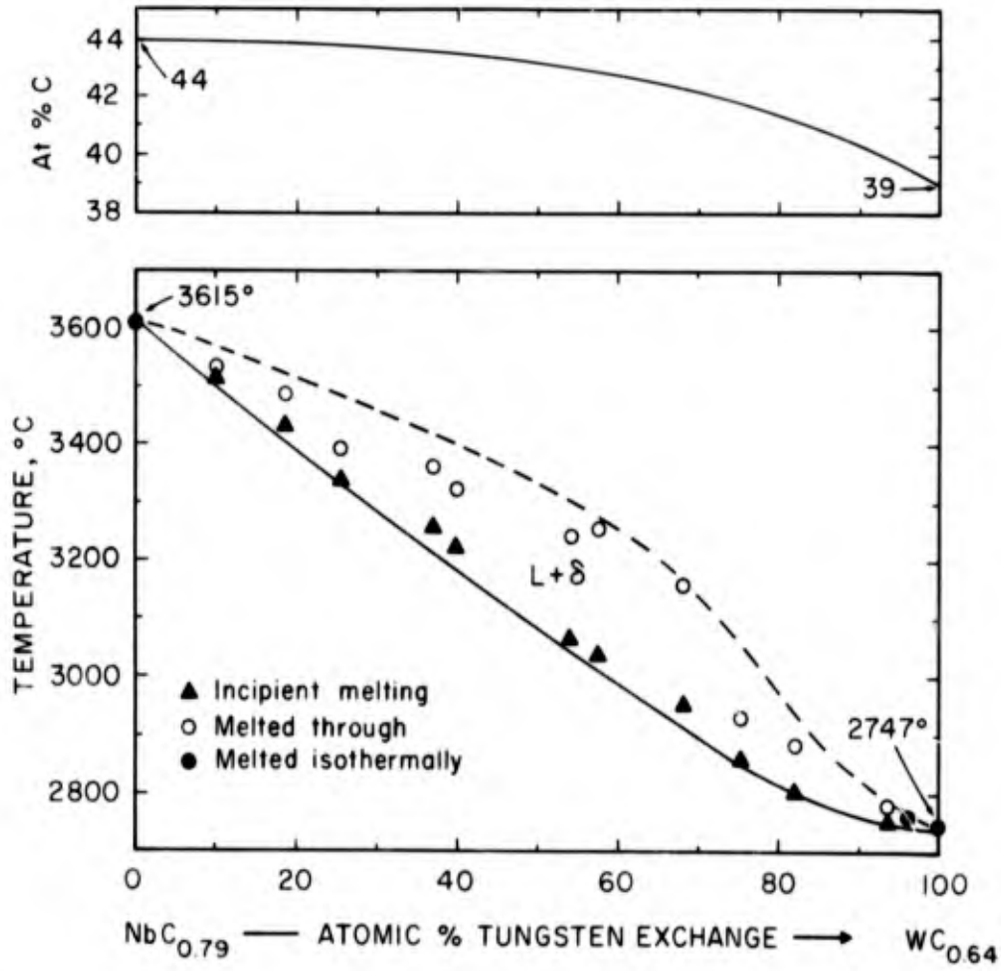

Figure 30. Maximum Solidus Temperatures of the Monocarbide, $(Nb, W)C_{1-x}$ Solid Solution.

Top: Line of the Maximum Solidus.

Monocarbide alloys which were quenched or rapidly cooled from liquidus temperatures were heavily cored and the diffraction patterns of these alloys were correspondingly diffuse. To obtain homogeneous alloys for X-ray studies, the alloys were, after melting, homogenized for 1 to 2 minutes at slightly subsolidus temperatures, and then rapidly cooled to room temperatures. After this treatment, the X-ray patterns of the majority of alloys were sharp and the samples proved to be homogeneous under the microscope (Figure 31). Exceptions were only encountered in specimens located near the tungsten-carbon binary, where the rapid disproportionation of the monocarbide phase resulted in the occurrence of non-equilibrium mixtures of cubic monocarbide, tungsten monocarbide, and subcarbide phase at intermediate cooling rates (Figure 32).

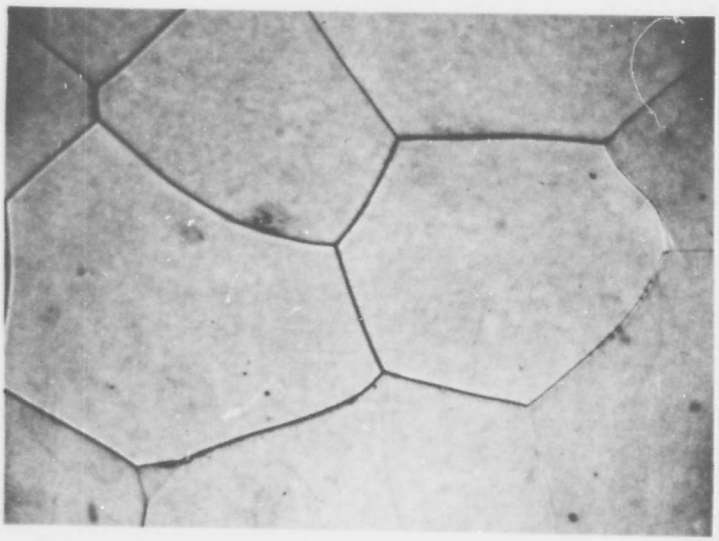

Figure 31. Nb-W-C (30-22-48 At.%), Rapidly Cooled Following Equilibration at 3100°C. X700

Single Phase Monocarbide.

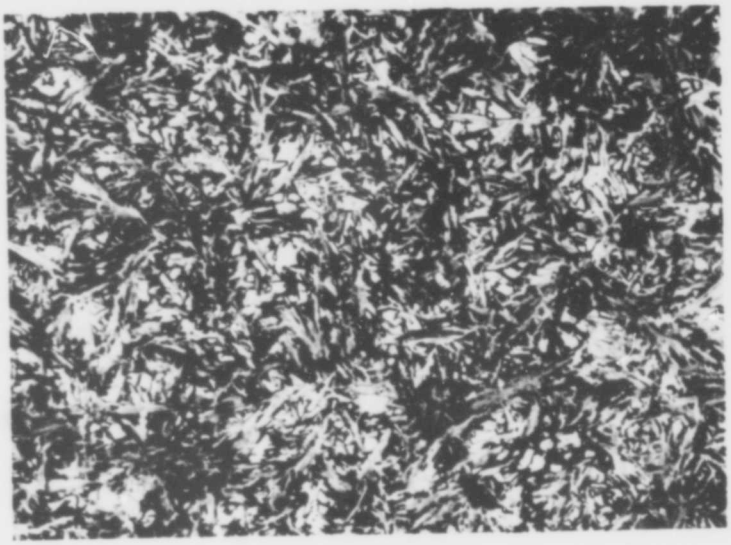

Figure 32. Nb-W-C (2-58-40 At.%), Cooled at ~100°C Per Second from 2750°C. X400

Monocarbide Solid Solution (Decomposed), with Small Amounts of Excess Tungsten Monocarbide.

In spite of the large differences of the eutectic temperatures in the carbon-rich regions of both binary systems, melting in the alloys located along the monocarbide + graphite eutectic trough did not appear too heterogeneous (Figure 33); correspondingly, the microstructures of melted alloys were found to resemble closely those of binary eutectics, instead of showing the morphology typical for bivariant solidification.

The course of the eutectic trough itself was delineated by microscopic inspection of the as-melted and quenched alloys. Typical examples of microstructures of melted alloys located at, or near, the monocarbide + graphite eutectic trough are depicted in Figures 34 through 37.

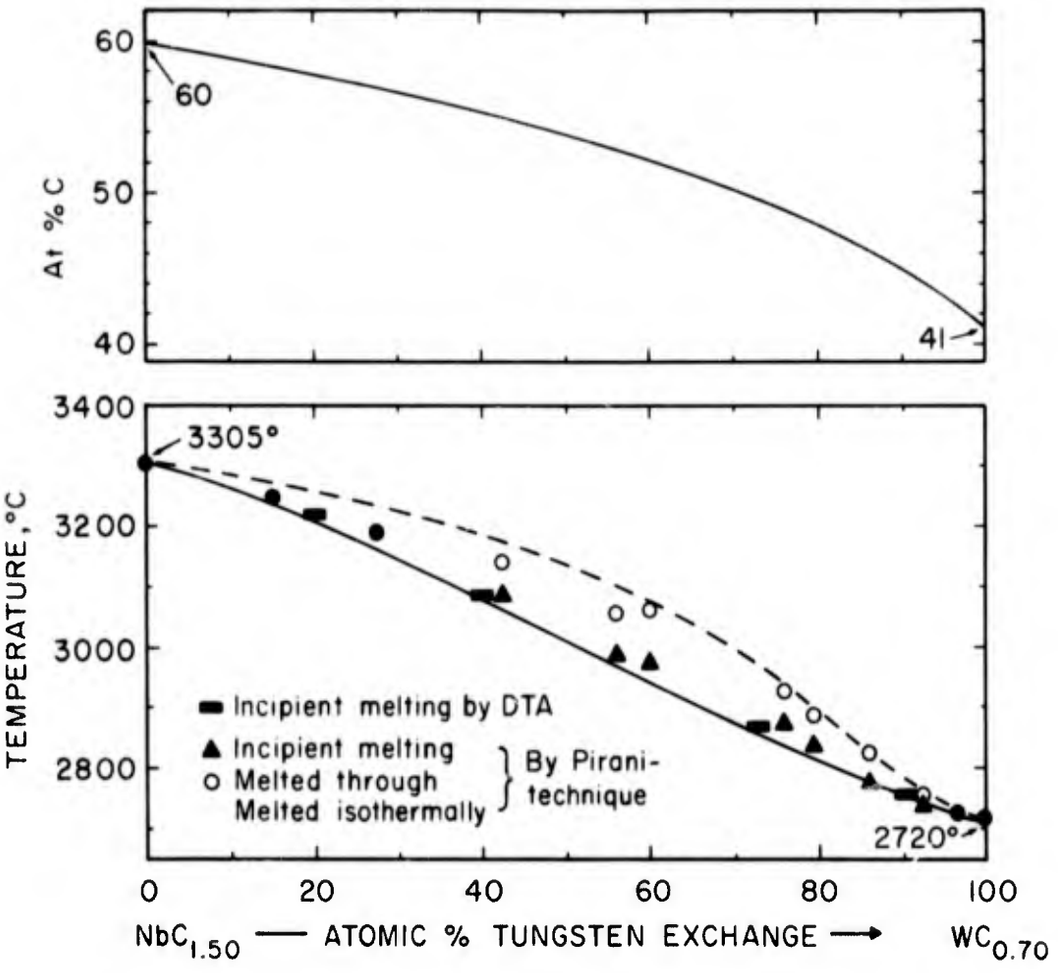

Figure 33: Melting Along the (Nb, W)C_{1-x} + C Eutectic Trough.

Top: Metallographically Estimated Course of the Eutectic Trough.

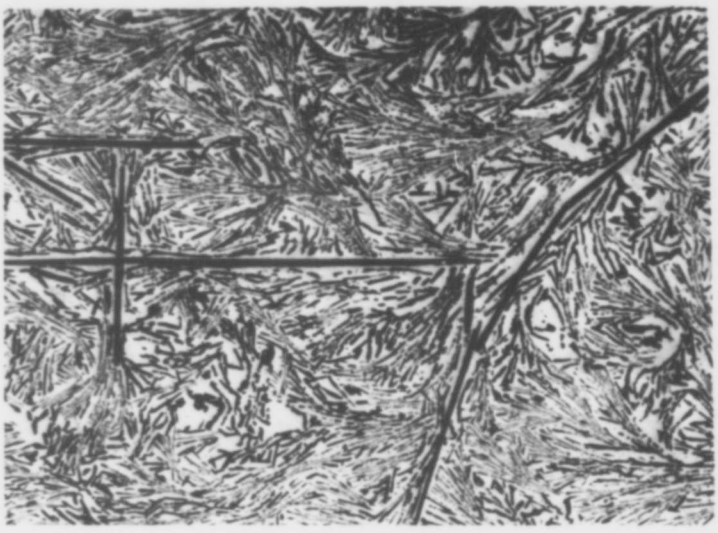

Figure 34. Nb-W-C (34-6-60 At.%), Rapidly Cooled From ~3300°C. X130

Small Amounts of Primary Graphite in Monocarbide + Graphite Eutectic Matrix.

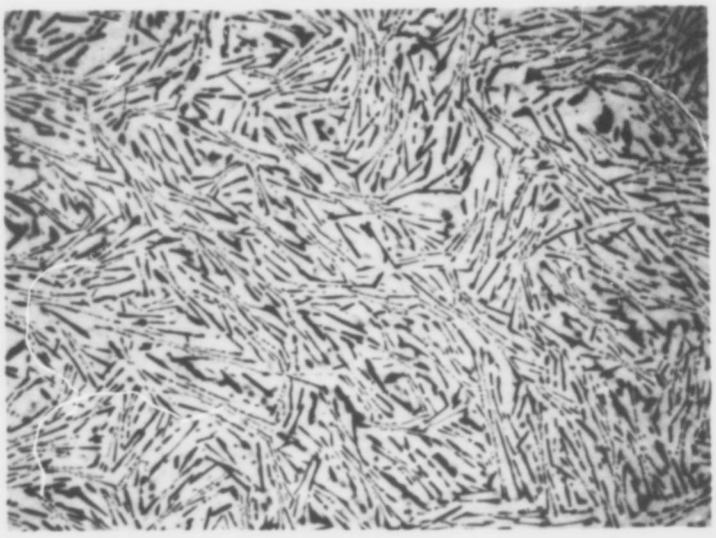

Figure 35. Nb-W-C (33-11-59 At.%), Melted and Rapidly Cooled X400

Monocarbide + Graphite Eutectic-Type Structure.

Figure 36. Nb-W-C (27-20-53 At.%), Melted and Rapidly Cooled. X275

Primary Monocarbide in a Eutectic-Like Matrix of Monocarbide + Graphite.

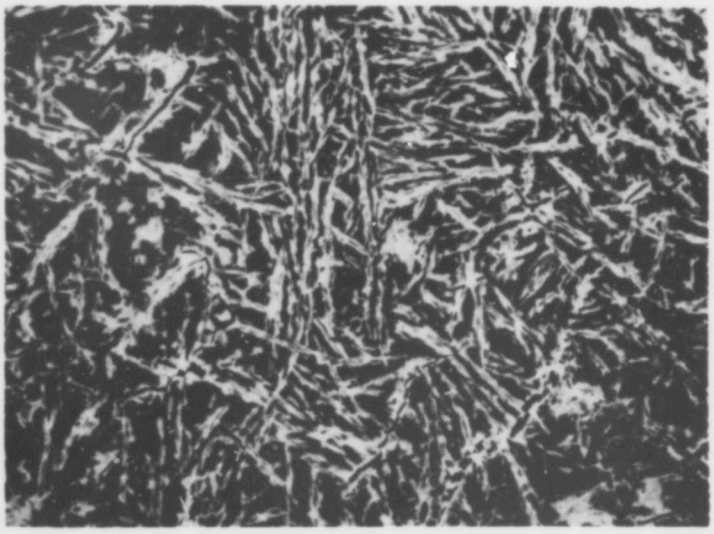

Figure 37. Nb-W-C (4-46-50), Melted and Rapidly Cooled X350

Primary Graphite with Peritectic-Type Walls of Tungsten Monocarbide, and a Eutectic Matrix of α-WC_{1-x}-ss + WC (Monocarbide Phase Decomposed).

3. Assembly of the Phase Diagram

The experimental data have been combined to develop the temperature sections of the Nb-W-C system depicted in Figures 38 through 41. From these sections, as well as the experimental liquidus projections (Figure 3) and the experimental data gathered on selected concentration sections, a phase diagram of the system for temperatures above 1500°C was constructed (Figure 1). This diagram is supplemented by the flow scheme of isothermal reactions depicted in Figure 2 as well as by an isopleth at $NbC_{0.47}$-$WC_{0.47}$ which is shown in Figure 4.

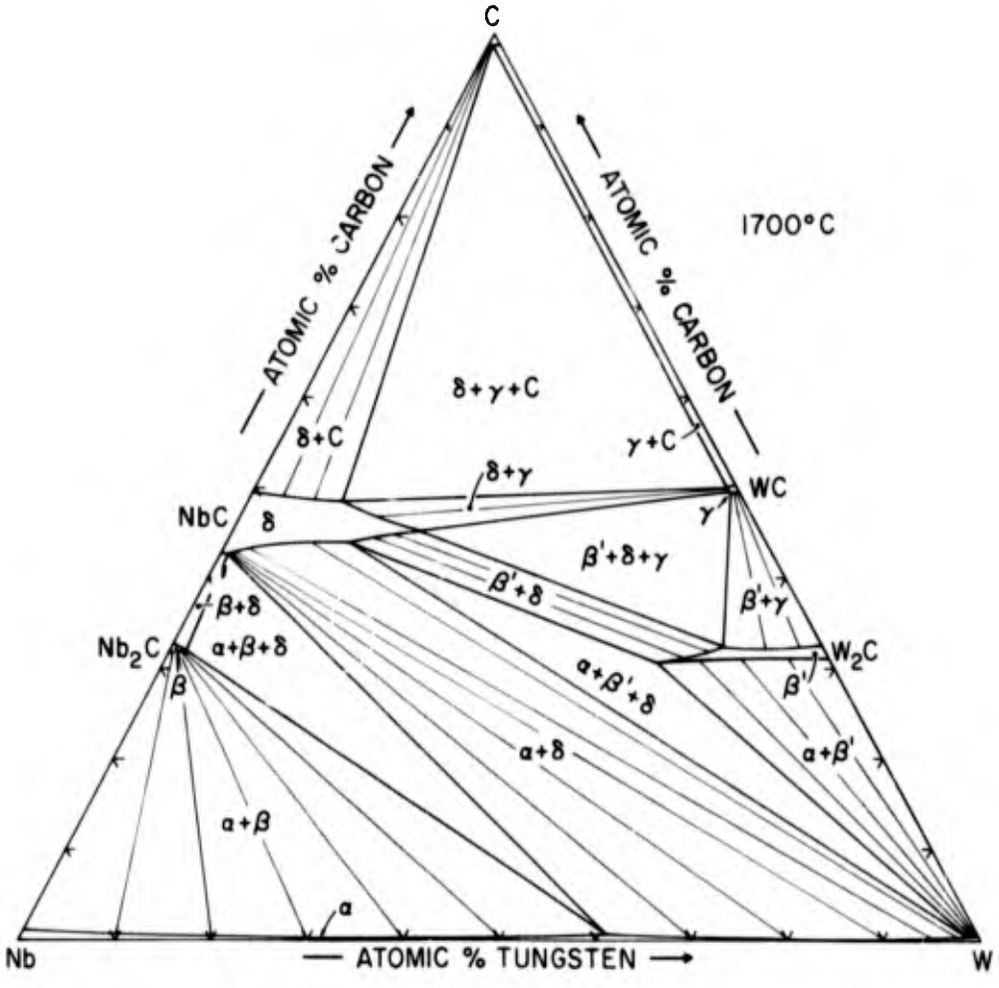

Figure 38. Isothermal Section at 1700°C.

The continuation of the phase transition in the Me_2C-phases into the ternary phase field was not studied in detail; specifically, it was not possible from our experiments to ascertain how far the two-phased transitions reach into the ternary and by what type of reaction these two-phased processes are terminated. The only conclusions which can be drawn from DTA-experiments on Nb_2C-rich as well as on W_2C-rich alloys are that the apparent transition temperatures of both binary subcarbides are lowered by the mutual metal exchange. Since the effect of these transitions upon the phase relationships is only secondary, they were disregarded in the layout of the phase diagram.

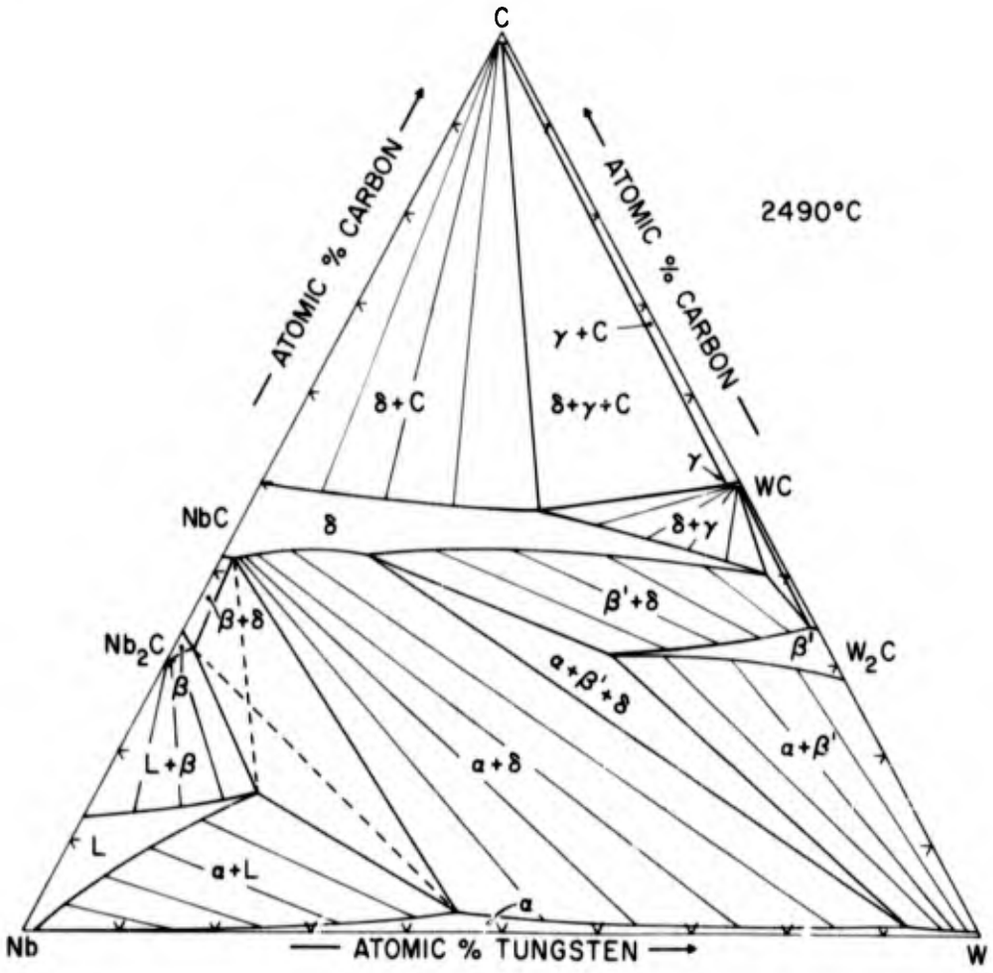

Figure 39. Isothermal Section at 2490°C.

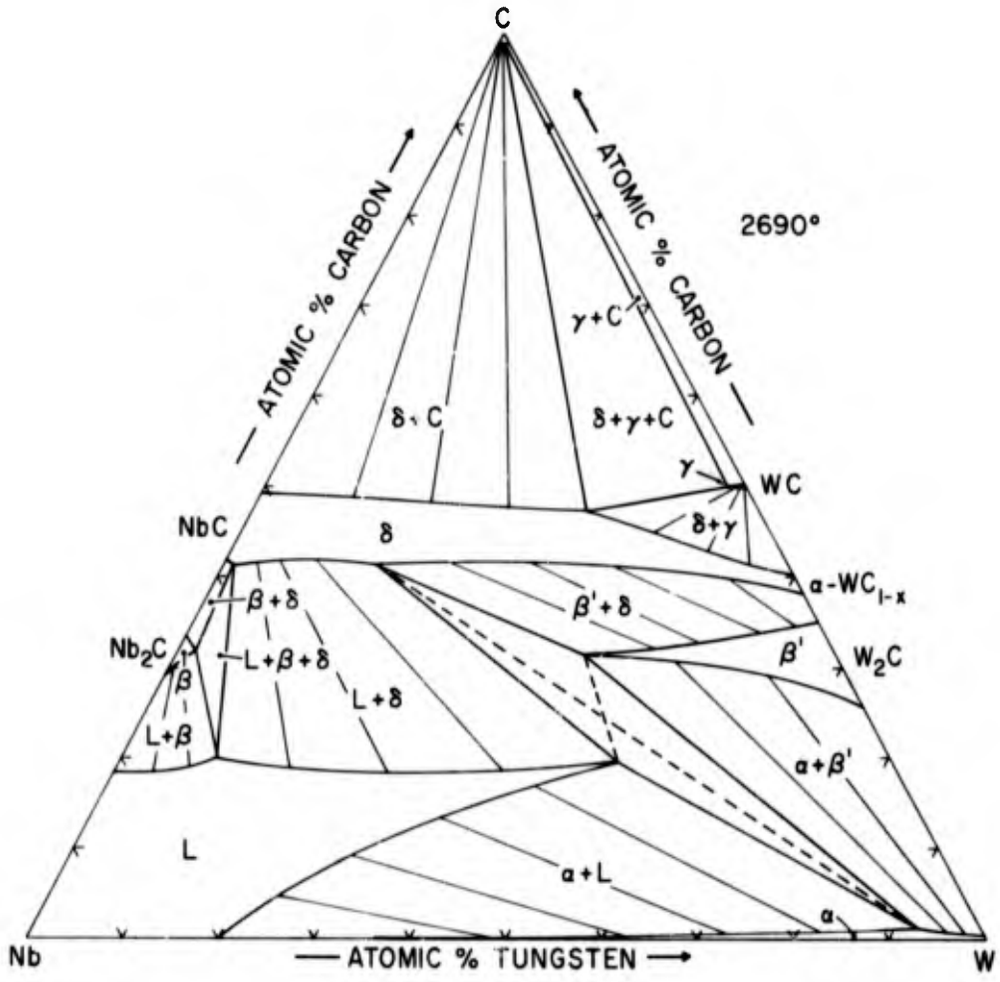

Figure 40. Isothermal Section at 2690°C.

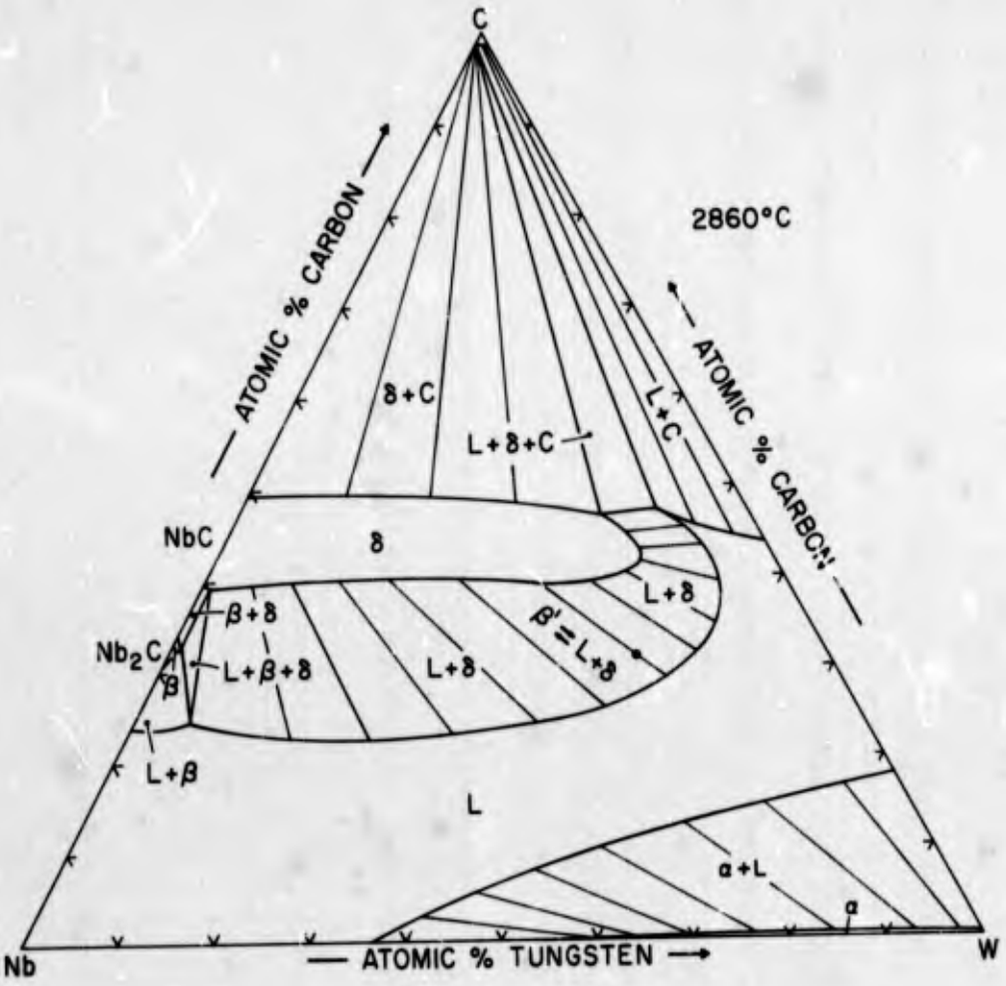

Figure 41. Isothermal Section at 2860°C.

V. DISCUSSION

The general phase diagram features of the niobium-tungsten-carbon are very similar to those of the Nb-Mo-C system established previously[1,2]; such a behavior becomes understandable, since previous thermodynamic analysis of related systems[2,3,5] identified the relative stabilities of the Me_2C-phases as the most important factor in the appearance of the phase equilibria in the metal-rich regions of these systems. These relative stabilities are about the same for Mo_2C and W_2C and hence whatever differences do exist will mainly be attributable to the differences between the stability of monocarbide and subcarbide phases in both binary Group V metal-carbon systems and only secondarily by eventual differences in the solution behavior.

To evaluate the phase relationships in the Nb-W-C system thermodynamically, we follow the same approaches as outlined previously[2,3,5]. Under the assumptions of this simplified treatment, namely that the free energies of the metal carbide solutions are allowed to vary only with the metal-exchanges, the conditional equations governing the tie line distributions within any two-phase field $(A, {}_{x'_A}, B_{x'_B})C_u + (A_{x''_A}, B_{x''_B})C_v$ is given by[42]:

$$\left[\frac{\partial \Delta G_{f,(A,B)C_u}}{\partial x'}\right]_{T,p} = \left[\frac{\partial \Delta G_{f,(A,B)C_v}}{\partial x''}\right]_{T,p} \qquad (1)$$

$\Delta G_{f,(A,B)C_u}$ and $\Delta G_{f,(A,B)C_v}$ are the free enthalpies of formation of the solid solutions $(A,B)C_u$ and $(A,B)C_v$ respectively, and x' and x'' are the mole fractions of A, or B, on the sublattices of the solutions $(A,B)C_u$ and $(A,B)C_v$.

The appearance of three-phase equilibria is governed by two sets of equations; the first relates to the fact that the gradient condition for the two-phase equilibrium has to be fulfilled for all three adjoining two-phase equilibria, i.e. we obtain three sets of relations of the form of equation (1). The second set relates to the free enthalpy (p = const.) balance between the three coexisting phases and correspondingly is referred to as stability condition[42]:

$$\Delta G_{Z,AC_v} + \overline{\Delta G}^{mix}_{Z,AC_v} = \phi_Z \qquad (2a)$$

and

$$\Delta G_{Z,BC_v} + \overline{\Delta G}^{mix}_{Z,BC_v} = \phi_Z \qquad (2b)$$

$\Delta G_{Z,AC_v}$ and $\Delta G_{Z,BC_v}$ are the free enthalpies of disproportionation of the binary phases AC_u and AC_v according to:

$$(w-u)\ A(B)C_u \rightarrow (w-v)\ A(B)C_u + (v-u)\ A(B)C_w \ldots . \Delta G_{Z,A(B)C_v},$$

and the terms $\overline{\Delta G}^{mix}_{Z,A(F)C_v}$ abbreviate the sum of the mixing terms according to the same reaction scheme. The quantity ϕ_Z corresponds to the integral free enthalpy of the disproportionation of the phase solution $(A,B)C_v$ into the neighboring solutions $(A,B)C_u$ and $(A,B)C_w$. ϕ_Z is zero for the case of equilibrium; for $\phi_Z > O$, the solution $(A,B)C_v$ is stable, whereas for $\phi_Z < O$ single phased alloys $(A,B)C_v$ are unstable.

The thermodynamic data for the niobium- and the tungsten carbides (Tables 4 and 5) are substantially the same as those used in previous phase-diagram calculations[2, 3, 5]. These data are based on compilations by E.K. Storms[43], H.L. Schick[44], and Y.A. Chang[45], as well as on values which have been back-calculated from experimentally established phase diagram information[4, 42].

Table 4. Free Enthalpy Data for Niobium Carbides (T > 1500°C)

Reactions	Free Enthalpy of Formation or Reaction (cal/gr.-At.Nb; Temperature in °K)
$Nb + 0.71C \rightarrow NbC_{0.71}$	$\Delta G_f = -27,350 + 0.833 \cdot T$
$Nb + 0.75C \rightarrow NbC_{0.75}$	$\Delta G_f = -28,250 + 0.807 \cdot T$
$NbC_{0.485} \rightarrow 0.65\ NbC_{0.75} + 0.35 \cdot Nb$	$\Delta G_{Z,NbC_{0.485}} = 1,982 - 0.54 \cdot T$

Table 5. Free Enthalpy Data for Tungsten Carbides (T > 1500°C)

Reaction	Free Enthalpy of Formation or Reaction (cal/gr.-At. W; Temperatures in °K)
$W + C \rightarrow WC$ (hex)	$\Delta G_{f, WC} = -8{,}900 + 0.48 \cdot T$
$W + 1/2\ C \rightarrow WC_{1/2}$	$\Delta G_{f, WC_{1/2}} = -3{,}150 - 0.62 \cdot T$
$W + C \rightarrow WC$ (B1)	$\Delta G_{f, WC_{1.0}} = -3.750 - 0.95 \cdot T$
$W + 0.71C \rightarrow WC_{0.71}$ (B1)	$\Delta G_{f, WC_{0.71}} = -730 - 1.88 \cdot T$
$W + 0.61C \rightarrow WC_{0.61}$ (B1)	$\Delta G_{f, WC_{0.61}} = +340 - 2.08 \cdot T$
WC_{1-x} (B1) $\rightarrow (1-2x)$ WC(hex) + $2x\ WC_{1/2}$	$\Delta G_{Z, WC_{1-x}(cub)} = -4800 + 1.71 \cdot T$ $(0.08 \leq x \leq 0.35)$

Assuming, as a first approximation, ideal behavior of all solutions, we obtain with these thermodynamic data the following equations for the free enthalpy-concentration gradients for the three solutions (Nb, W), $(Nb, W)_2C$, and $(Nb, W)C_{1-x}$.

$$\frac{1}{4.574 \cdot T} \cdot \left[\frac{\partial \Delta G_{f, (Nb, W)}}{\partial x'}\right]_{T, p} = \log \frac{x'}{1-x'} \qquad (3a)$$

$$\frac{1}{4.574 \cdot T} \cdot \left[\frac{\partial \Delta G_{f, (Nb, W)C_{1/2}}}{\partial x''}\right]_{T, p} = \frac{3{,}760}{T} - 0.367 + \log \frac{x''}{1-x''} \qquad (3b)$$

$$\frac{1}{4.574 \cdot T} \cdot \left[\frac{\partial \Delta G_{f, (Nb, W)C_{0.75}}}{\partial x''}\right]_{T, p} = \frac{5{,}910}{T} - 0.56 + \log \frac{x'''}{1-x'''} \qquad (3c)$$

x', x'', x''': Mole fractions of tungsten on the metal (sub) lattice of (Nb, W), $(Nb, W)_2C$, and $(Nb, W)C_{0.75}$.

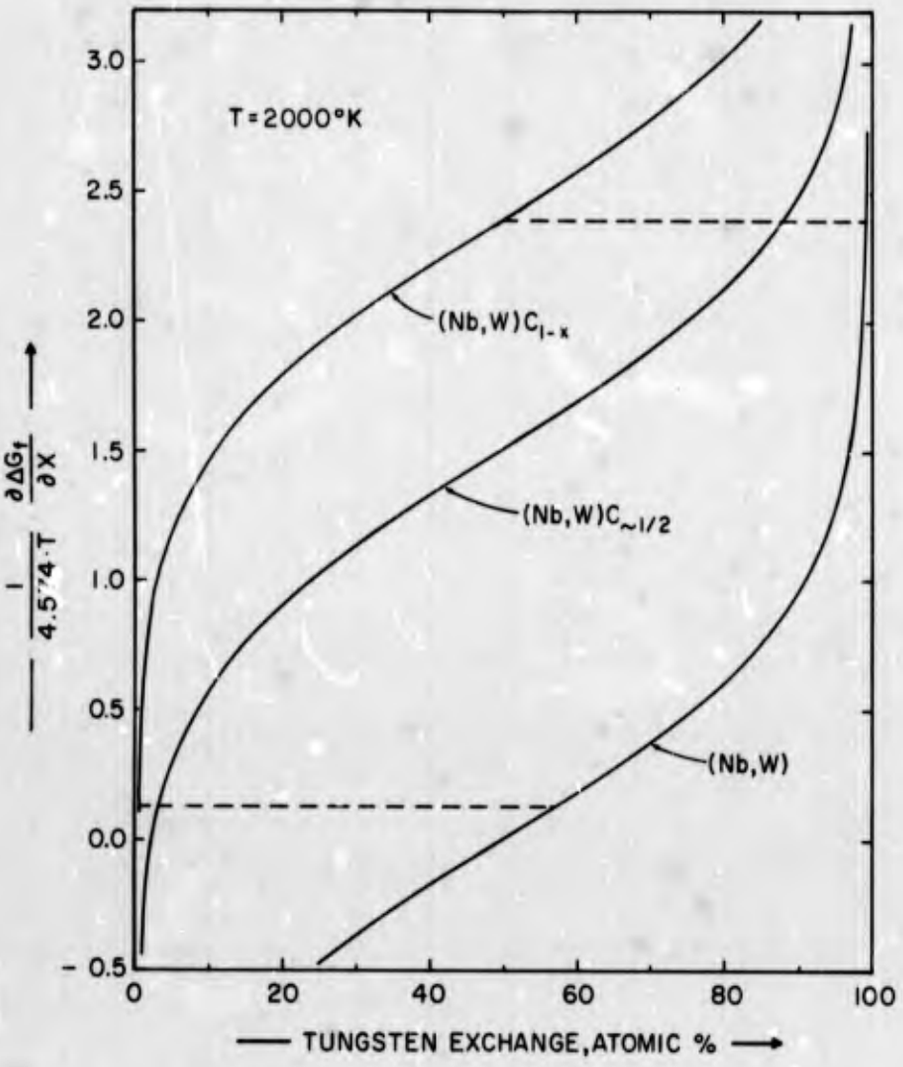

Figure 42. Free Enthalpy-Concentration Gradient Curves for Niobium-Tungsten and Niobium and Tungsten Carbide Solid Solutions. T = 2000°K.

(Dashed Curves Indicate Composition of Coexisting Three Phases).

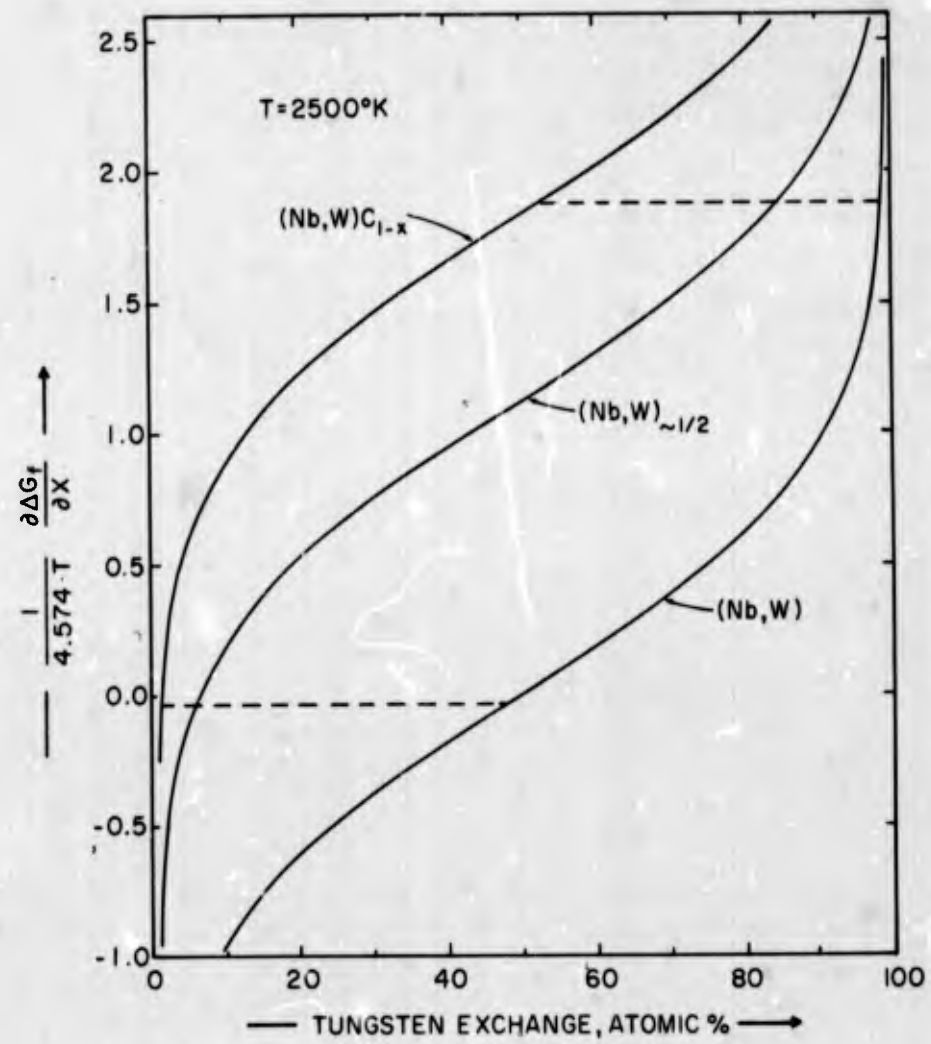

Figure 43. Free Enthalpy - Concentration Gradient Curves. T = 2500°K. (Dashed Curves Indicate Composition of Coexisting Three Phases).

The expressions (3a) through (3c) for the gradients can be combined according to equation (1) to yield the equilibrium constants for the three two-phase equilibria possible between the three phase solutions; as a rule, however, and this applies especially to the case where nonideal solutions are to be considered, it is more convenient to solve the equations graphically by plotting the free enthalpy gradients versus the compositions; for the selected equilibrium temperature, the coexisting phase compositions (i.e. the end points of the tie lines) are obtained as the horizontal intercepts of these gradient curves. Two such plots, for 2000 and 2500°K, are depicted in Figures 42 and 43.

The Z-function for a disproportionation of subcarbide, $(Nb, W)_2C$, solid solution into solutions of metal alloy, (Nb, W) and monocarbide $(Nb, W)C_{1-x}$ according to:

$$MeC_{0.48} \rightarrow 0.65\ MeC_{0.75} + 0.35\ Me$$

can be written as

$$\phi_Z = \Delta G_{Z,\,MeC_{1/2}} + 4.574 \cdot T \frac{x'''^{0.65}_{Me} \cdot x'^{0.35}_{Me}}{x''_{Me}} \qquad (4)$$

where Me stands for either niobium or tungsten; using x''_W, i.e. the mole fraction of tungsten in the metal sublattice of the subcarbide phase as the running variable, the corresponding composition x'_W and x'''_W are either obtained from the gradient curves, Figures 42 and 43, or are calculated directly from equations (3a) through (3c). ϕ_Z is tnen computed with the aid of equation (4).

Carrying out these calculations, it is seen from the plot in Figure 44 that the relative stability of the subcarbide phase increases somewhat with increasing temperature, but not quite enough as to allow the formation of a complete solid solution within the solidus range.

For the other three-phase areas to be considered in the calculations, namely the equilibria

$$(Nb, W)C_{1-x}\ (cub) + W_2C\text{-ss} + WC\ (hex)\text{-ss}$$

and

$$WC\ (hex)\text{-ss} + (Nb, W)C_{1-x}\text{-ss} + C,$$

it is seen from a comparison of the thermodynamic quantities, or from a plot of the corresponding gradient curves, that the WC(hex)-vertex of the first-mentioned three-phase equilibrium lies very close to the binary phase and, therefore, the solution terms for this phase can be neglected. Similarly, as a result of the comparatively high free energies of transformation of the cubic (B1) NbC into a monocarbide having the WC-structure, the maximum niobium exchange in WC is very small and can, to a first approximation, be neglected in the calculations.

Under these conditions, the stability conditions for the above two, three-phase equilibria become:

(a) For the equilibrium $(Nb,W)C_{1-x}(cub) + W_2C\text{-ss} + WC(hex)\text{-ss}$:
(Reaction $WC_{1-x}(B1) \rightarrow a \cdot WC + b\ WC_{1/2}$)

$$\phi_{Z,(Nb,W)C_{1-x}} = \Delta G_{Z,\,WC_{1-x}} + RT \ln \frac{x'(b)}{x''} \qquad (5)$$

The exponent b, which depends on the stoichiometry of the equilibrium phases, varies between 0.26 at 2000°K and 0.71 at 3000°K. Using x''_W, the mole fraction of tungsten on the metal sublattice in the cubic monocarbide phase, as the running variable, the coexisting subcarbide compositions can, as described before, be obtained from the gradient curves, and $\phi_{Z(Nb,W)C_{1-x}}$ evaluated with the aid of equation (5). Carrying out the calculation, we obtained the following equilibrium concentrations (x'''_W in WC ≈ 1)

The maximum metal exchanges in Nb_2C and W_2C at a given temperature are given by the condition that $\phi_Z = \emptyset$, and can be seen (Figure 44) to increase somewhat with temperature. The phase compositions determined by $\phi_Z = \emptyset$ also form the Me_2C-vertex of the three-phase equilibrium $Me + Me_2C + MeC_{1-x}$, which restrains the subcarbide phases towards the ternary; the other two vertices, of each three-phase equilibrium, at the metal and monocarbide phase, are obtained directly from the gradient curves.

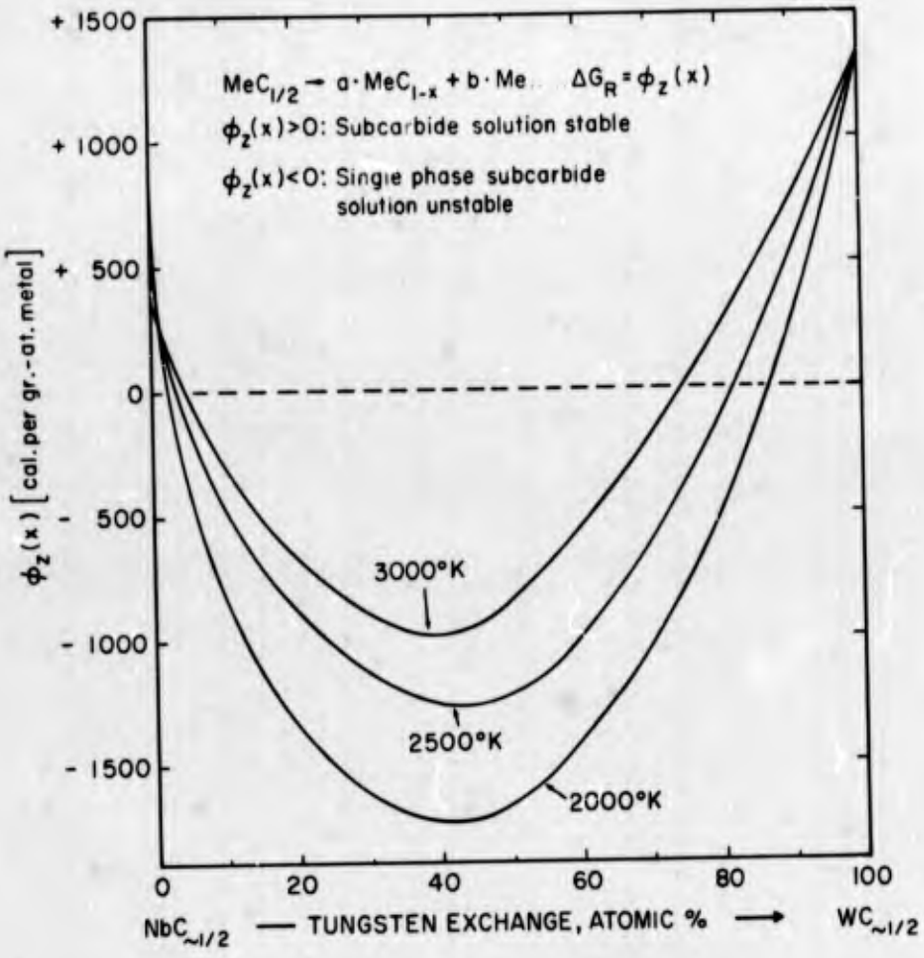

Figure 44. Integral Free Enthalpy of Disproportionation of the Subcarbide, $(Nb, W)_2C$, Solid Solution into Monocarbide, $(Nb, W)C_{1-x}$, and Metal, (Nb, W), Solid Solutions.

Temperature	x'_W	x''_W
2000°K	0.94	0.70
2500°K	0.96	0.87

(b) For the equilibrium $(Nb, W)C_{1-x}$(cub) + WC(hex) + C
(x_C in C ~ 1; x''_W in WC ~ 1)

$$\log x'_W = -\frac{1,130}{T} + 0.311$$

Insertion of the equilibrium temperatures into the above equations yields for x'_W, the mole fraction of tungsten in the metal sublattice of the monocarbide, values of 0.63 and 0.72 and 2000° and 2500°K, respectively.

The calculated equilibrium compositions can now be used to delineate the various two- and three-phase areas in the system. The tie lines in the two-phase fields are obtained, as discussed before, from the gradient curves. Two isotherms, at 2000°K and 2500°K were assembled from the calculated data and are depicted in Figures 45 and 46.

A comparison of the experimental with the theoretical phase diagram sections shows that the gross features of the system are reproduced fairly well by the calculations, especially as far as the equilibria in the metal-rich region are concerned. The agreement between the calculated and the measured metal-exchanges in the cubic monocarbide phase, as well as the B1-vertex of the three-phase equilibria $(Nb, W)C_{1-x}$(B1) + WC + C is less good, especially at the lower temperatures. The discrepancies—the calculated solubilities in the monocarbide area tend to be higher than the experimental, and the calculated equilibrium constants in the two-phase fields Me + MeC_{1-x}(B1) and Me_1C-MeC_{1-x}(B1) are smaller than those observed—indicate a significant deviation of the monocarbide solution from ideality. Such a behavior has indeed been deduced from back-calculations, using experimentally established solubility curves for the systems (Nb, Ta)C-WC[4]. Treating, as a first approximation, the phases as regular solutions, interaction parameters of

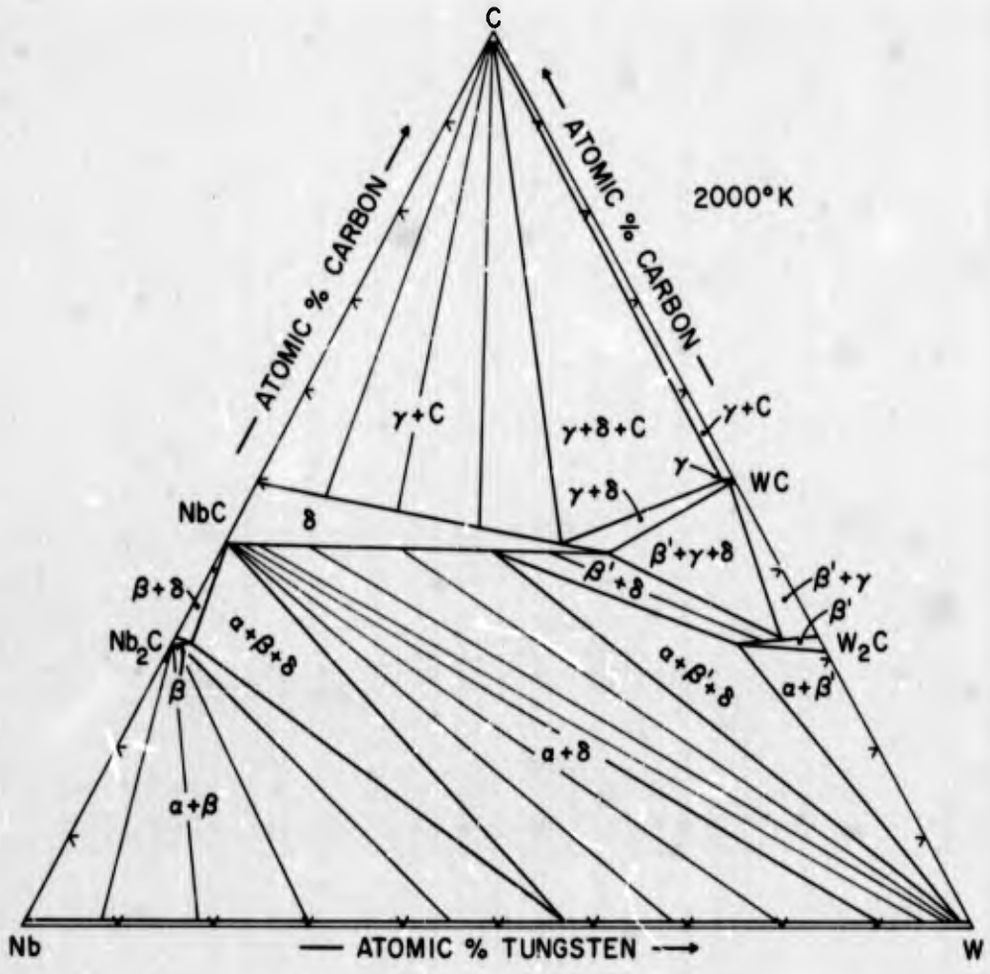

Figure 45. Calculated Isothermal Section at 2000°K.

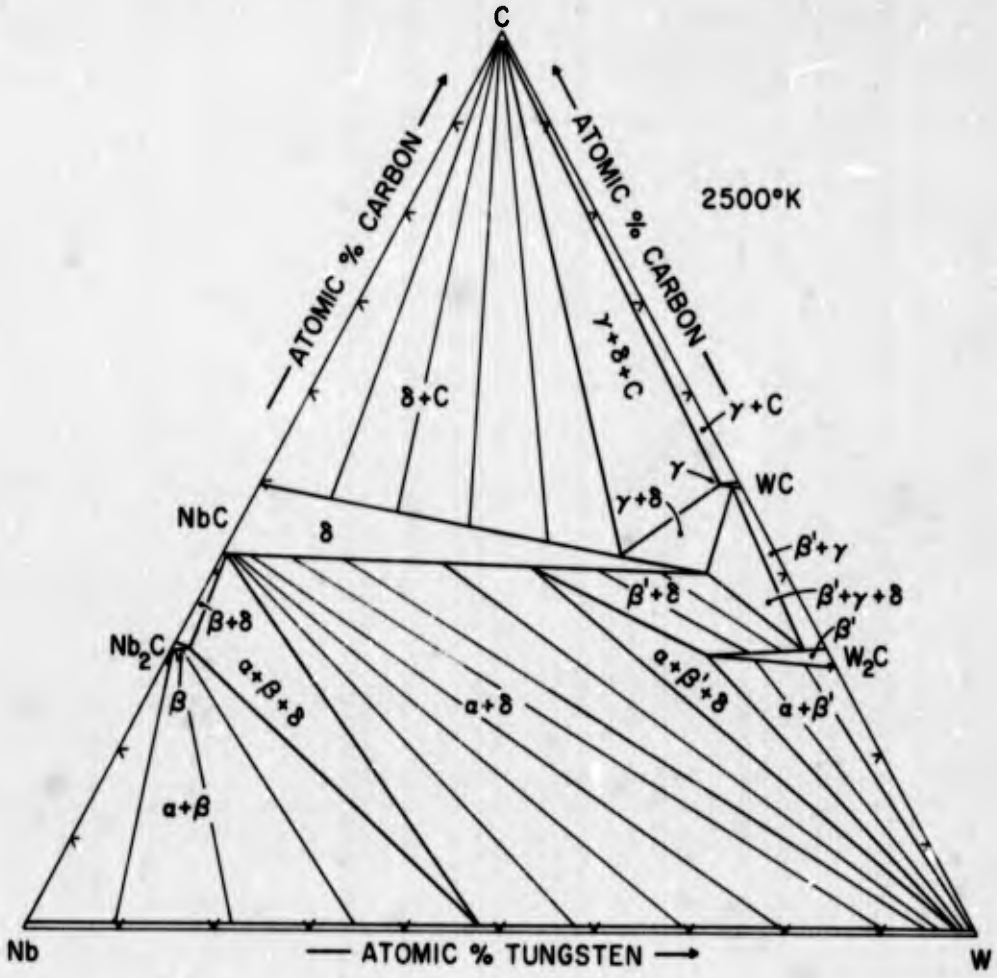

Figure 46. Calculated Isothermal Section at 2500°K.

of ϵ = + 6500 cal/gr.-At. metal were obtained for the carbon-saturated monocarbide phases (Nb, W)-(Mo, W)C_{1-x}. Taking the nonideal behavior into account in the calculations yields compositions for the equilibrium phases in the Nb-W-C system[46] which agree within $\pm$ 5 At.% with the experimental equilibrium compositions determined in this work.

REFERENCES

1. E.Rudy, F.Benesovsky, and K.Sedlatschek: Mh.Chem. 92 (1961), 841.

2. E.Rudy, C.E. Brukl, and St. Windisch: AFML-TR-65-2, Part II, Vol.XV (July 1967), Trans. AIME 239 (1967), 1796.

3. E.Rudy, St. Windisch, and C.E. Brukl: AFML-TR-65-2, Part II, Vol.XVII (August 1967). J.Amer. Ceram. Soc. (in print).

4. E.Rudy and Y.A. Chang: Papers presented at the V. Plansee Seminar 1964 (Plansee Proc. 1964, 786).

5. E. Rudy: AFML-TR-65-2, Part II, Vol.VIII (March 1966).

6. E.Rudy, El.Rudy, and F.Benesovsky: Mh.Chem. 93 (1962), 1176.

7. E.Rudy, El.Rudy, and F.Benesovsky: Planseeber, Pulvermet. 10 (1962), 42.

8. E. Rudy, F. Benesovsky, and El.Rudy: Mh.Chem. 93 (1962), 693.

9. Compare, for example, R.Kieffer and F. Benesovsky: Hartstoffe and Hartmetalle (Wien, Springer, 1963).

10. H. Buckle: Z. Metallkde 37 (1946), 53.

11. B.I. Krimer and Yu.E. Matveev: Moscow Steel Inst. 38 (1958), 420.

12. Y.S. Mikheev and D.M. Pevtsov: Zh.Nerog.Khim. 3 (1958), 861.

13. R.Kieffer, K. Sedlatschek and H. Braun: J.Less-Common Met. 1 (1959), 19; Z.Metallkde 50 (1959), 18.

14. Compare also the data compilation in:

    (a) M. Hansen, "Constitution of Binary Alloys" (McGraw-Hill, New York, 1958).

    (b) R.P. Elliott, "Constitution of Binary Alloys, First Supplement" (McGraw-Hill, New York, 1965).

    (c) W.B. Pearson, "Lattice Spacings and Structures of Metals and Alloys", [Pergamon, New York, Vol.1 (1958), Vol.II (1967)] ∞

15. E.K. Storms and N.H. Krikorian: J.Phys.Chem. 64 (1960), 1471.

16. H. Kimura and Y.Sasaki: Trans.Jap.Inst.Met. 2 (1961), 98.

17. E. Rudy, St. Windisch, and C.E. Brukl: AFML-TR-65-2, Part I, Vol.XII (Sept. 1967), Planseeber. Pulvermet. (in print).

18. E.Rudy and C.E. Brukl: J.Amer.Ceram. Soc. 50, No.5, (1967), 265.

19. N. Terao: Jap. J. Appl. Phys. 3 (1964), 104.

20. N.M. Volkova and P.V. Gel'd: Izvest. Vysh. Uchebnik Zaved. Tsvetnaya Metallurgiya 3 (1965), 77.

21. S.I. Alyamovskii, G.P. Sheikin, and P.V. Gel'd: J.Neorg.Chim. 8 (1963), 2000.

22. K. Yvon, H.Nowotny, and R.Kieffer: Mh.Chem. 98 (1967), 34.

23. E.Rudy: AFML-TR-65-2, Part II, Vol.VIII (March 1966), p.105.

24. E.Rudy, St. Windisch, and J.R. Hoffman: AFML-TR-65-2, Part I, Vol. VI (Jan 1966).

25. E. Rudy and J.R. Hoffman: Planseeber. Pulvermet. 15 (1967), 174.

26. R.T. Doloff and R.V. Sara: WADD TR 60-143 (1961), Part II.

27. R.V. Sara: J.Am. Ceram.Soc. 48 (5) (1965), 251.

28. E. Rudy and St. Windisch: J.Amer.Ceram. Soc. 50, No.5 (1967), 272.

29. G. Brauer and R. Lesser: Z. Metallkde 50 (1959), 8.

30. A. Westgren and G. Phragmen: Z.anorg. allg.Chem. 156 (1926), 27.

31. L.N. Butorina and Z.G. Pinsker: Soviet Physics, Crystallography, 5 (1960), 560.

32. K. Kimer, work quoted in (9).

33. A.G. Metcalfe: J. Inst. Met. 73 (1946), 591.

34. A.E. Kovalskii and J.S. Umanskii: Zhur.Fiz. Chim. 20 (1946), 773.

35. H.Nowotny and R.Kieffer: Metallforschung 2 (1947), 257.

36. C. Agte and H. Alterthum: Z.Techn. Phys. 11 (1930), 182.

37. A. Taylor and N.J. Doyle: J.Less Common Metals 13 (1967), 511.

38. M. Pirani and H. Alterthum: Z.Elektrochem. 29 (1923), 5.

39. E. Rudy and G. Progulski: Planseeber. Pulvermet. 15 (1967), 13. AFML-TR-65-2, Part III, Vol. II (May 1967).

40. H.D. Heetderks, E. Rudy, and T.E. Eckert: Planseeber.Pulvermet. 13 (1965), 105.

41. E.Rudy, St. Windisch, and Y.A. Chang: AFML-TR-65-2, Part I, Vol.I (Jan 1965).

42. E.Rudy: Part I, Z.Metallkde 54 (1963), 112-122;
Part II, Z.Metallkde 54 (1963), 213-223.

43. E.K. Storms: "The Refractory Carbides" (Academic Press, New York, 1967).

44. H.L. Schick: Thermodynamics of Certain Refractory Compounds, Vol.II (Academic Press, New York, 1966).

45. Y.A. Chang: USAF Tech.Doc. Rept. AFML-TR-65-2, Part IV. Vol.I (Sept. 1965).

46. Compare for example the predicted temperature section of the Nb-W-C system at 2000°K in the work cited under ref.42.

Unclassified
Security Classification

DOCUMENT CONTROL DATA - R & D

(Security classification of title, body of abstract and indexing annotation must be entered when the overall report is classified)

1. ORIGINATING ACTIVITY *(Corporate author)*

Materials Research Laboratory
Aerojet-General Corporation
Sacramento, California

2a. REPORT SECURITY CLASSIFICATION
Unclassified

2b. GROUP
N.A.

3. REPORT TITLE

Ternary Phase Equilibria in Transition Metal-Boron-Carbon-Silicon Systems
Part II. Ternary Systems.
Vol. XVIII. Constitution of Niobium-Tungsten-Carbon Alloys

4. DESCRIPTIVE NOTES *(Type of report and inclusive dates)*

5. AUTHOR(S) *(First name, middle initial, last name)*

Rudy, E.

6. REPORT DATE	7a. TOTAL NO. OF PAGES	7b. NO. OF REFS
January 1969	61	46

8a. CONTRACT OR GRANT NO.	9a. ORIGINATOR'S REPORT NUMBER(S)
AF 33(615)-1249	AFML-TR-65-2
b. PROJECT NO. 7350	Part II, Vol. XVIII
c. Task No. 735001	9b. OTHER REPORT NO(S) *(Any other numbers that may be assigned this report)*
d.	

10. DISTRIBUTION STATEMENT

This document has been approved for public release and sale; its distribution is unlimited.

11. SUPPLEMENTARY NOTES	12. SPONSORING MILITARY ACTIVITY
	AFML (MAMC) Wright-Patterson AFB, Ohio 45433

13. ABSTRACT

The ternary alloy system niobium-tungsten-carbon was investigated by means of X-ray, melting point, DTA, and metallographic techniques on chemically and thermally defined specimens. A phase diagram from 1500°C through the melting range was established.

The solid state equilibria in the system are characterized by limited metal exchanges in the subcarbides and the occurrence of a two-phase equilibrium between the monocarbide and the metal phase. Above 2530°C, niobium monocarbide and the cubic high temperature phase in the W-C system form an uninterrupted series of solid solutions; below this temperature, the tungsten exchange in NbC is temperature-dependent and decreases to approximately 25 At% W at 1500°C. The tungsten exchange in Nb_2C is less than 5 At% at all temperatures, whereas the solubility in W_2C increases from 24 mole% Nb_2C at 1500°C, to a maximum of approximately 37 mole% Nb_2C at 2600°C. The order-disorder reaction, as well as the change-of-order transition, temperature in W_2C and Nb_2C are lowered by niobium additions, but the details of the transition reactions in the ternary could not be delineated.

Five isothermal reactions, all of which involve a liquid phase, occur in the system. Two correspond to limiting tie lines and the remaining three are class II (two-over-two) ternary reactions.

The results of this phase diagram investigation are discussed and the phase equilibria thermodynamically analyzed and interpreted.

DD FORM 1 NOV 65 1473

Unclassified
Security Classification

14. KEY WORDS	LINK A		LINK B		LINK C	
	ROLE	WT	ROLE	WT	ROLE	WT
Ternary Phase Equilibria Carbides Thermodynamics						